JOURNAL OF GEOPHYSICAL RESEARCH, VOL. 100, NO. D8, PAGES 16,553–16,578, AUGUST 20, 1995

Preliminary study of spin-up processes in land surface models with the first stage data of Project for Intercomparison of Land Surface Parameterization Schemes Phase 1(a)

Z.-L. Yang and R. E. Dickinson

Institute of Atmospheric Physics, University of Arizona, Tucson

A. Henderson-Sellers and A. J. Pitman

Climatic Impacts Centre, Macquarie University, North Ryde, New South Wales, Australia

Abstract. The spin-up of a land surface model (LSM) is broadly defined as an adjustment process as the model approaches its equilibrium following initial anomalies in soil moisture content or after some abnormal environmental forcings (e.g., drought). The spin-up timescale of LSMs has received little attention in the modeling community. This study uses results from Phase 1(a) of the Project for Intercomparison of Land Surface Parameterization Schemes, and finds that most land surface schemes require many years to come to thermal and hydrologic equilibrium with the forcing meteorology; the time needed depends on the total moisture holding capacity and the initialization of the moisture stores. The linear relationship established for bucket-type models is just a special case of that found for the more sophisticated nonbucket-type models, at least when the models start out with adequate soil moisture. When soil moisture begins at zero or when precipitation is set to zero, there is a nonlinear relationship. Sensitivity studies using the Biosphere-Atmosphere Transfer Scheme confirm that precipitation intensity, solar radiation forcing, vegetation cover, and stomatal resistance also affect the length of spin-up time. The results underline that the accurate calculation of precipitation and solar radiation incident at the Earth's surface is important for a realistic simulation of soil moisture content. Magnitudes of simulated heat fluxes at equilibrium are not related to the thickness of the soil layer below the rooting zone. For most LSMs, initial positive soil moisture anomalies are associated with initial positive evapotranspiration (E) anomalies, while initial negative anomalies of soil moisture are accompanied by the initial negative, but much stronger, E anomalies, as found in past studies performed with general circulation models. In addition, the implications of the spin-up for numerical weather prediction and climate simulation are discussed.

1. Introduction

Land surface processes, including physical, ecological, and biogeochemical aspects, have received increasing attention in the climate system modeling community [*Trenberth*, 1992]. From a modeling point of view, the land acts as a lower boundary for approximately 30% of the atmosphere, exchanging moisture, momentum, heat, and trace gases. Also, from a practical viewpoint, land provides fresh water, crops, shelter, etc. for human requirements. From a viewpoint of global change, the impacts of climate on land surface conditions must be fully understood in order to plan for adaptation to climate change.

The World Meteorological Organization Commission for Atmospheric Sciences Working Group on Numerical Experimentation (WGNE) and the Science Panel of the Global Energy and Water Cycle Experiment Continental-scale International Project (GCIP) [*Chahine*, 1992] launched a joint WGNE/GCIP Project for Intercomparison of Land Surface Parameterization Schemes (PILPS) in 1992 [*Henderson-Sellers and Dickinson*, 1992; *Henderson-Sellers et al.*, 1993]. PILPS is also a diagnostic subproject of the WGNE Atmospheric Model Intercomparison Project (AMIP) [*Gates*, 1992] permitting intercomparison of coupled PILPS/AMIP models for the decade simulated by the AMIP groups. The principal goal of PILPS is to achieve a greater under-

Paper number 95JD01076.
0148-0227/95/95JD-01076$05.00

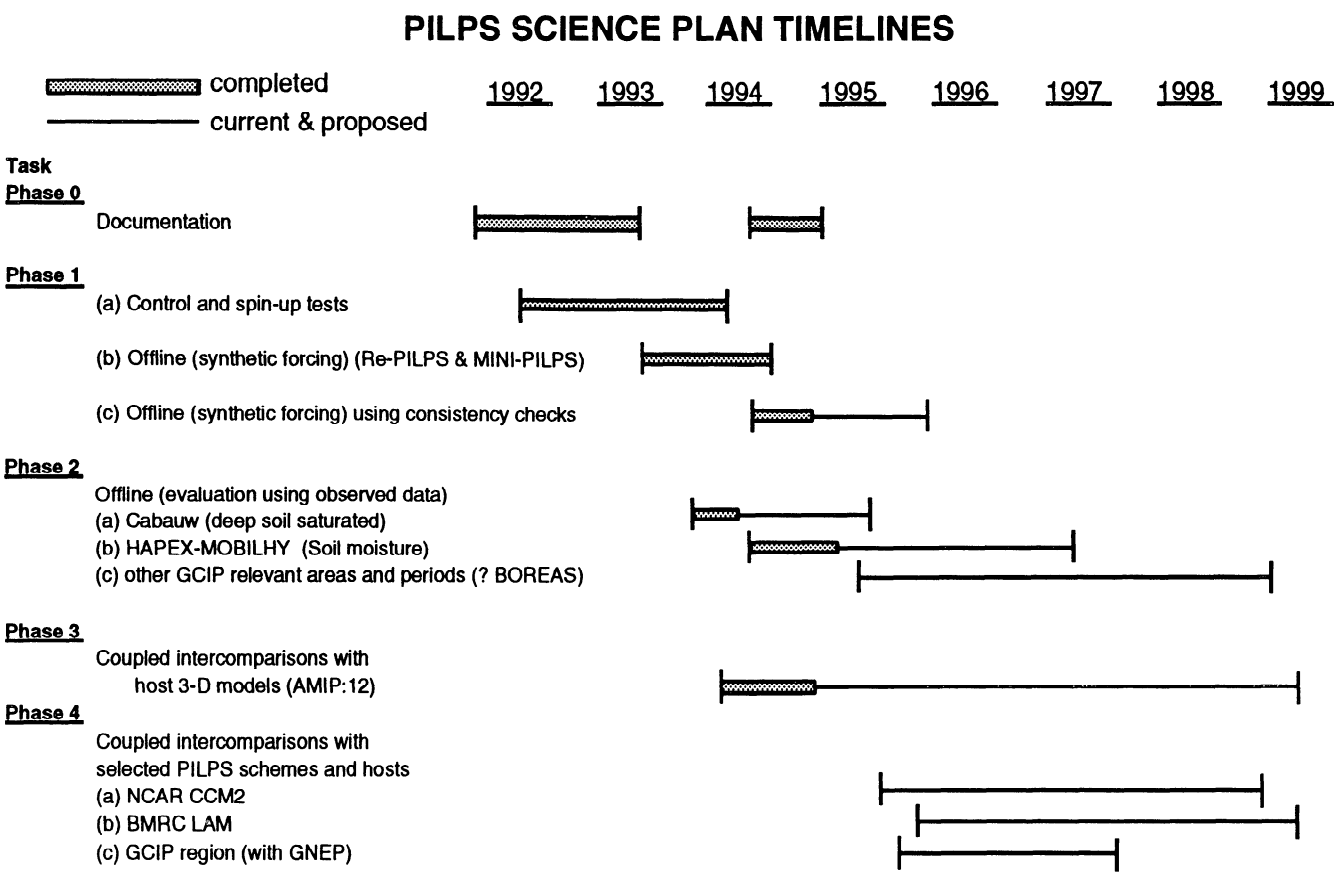

Figure 1. PILPS time lines.

standing of the capabilities and potential applications of both existing and new land surface schemes in atmospheric models (Figure 1).

The phases of the ongoing PILPS project are documented elsewhere [*Henderson-Sellers et al.*, 1993, 1995]. This paper focuses on the first stage of Phase 1(a) in which the same set of stand-alone simulations was performed by all of the participating models. Using atmospheric forcing data generated from a general circulation model (GCM), 22 participating land surface schemes (Tables 1a and 1b) were run to equilibrium. Forcing data for a tropical forest, a grassland, and a tundra grid point were used. The results from equilibrated states are documented by *Pitman et al.* [1993], in which it is noted that not all the participating schemes conserved moisture and energy properly: an incompleteness that is being revisited in PILPS Phase 1(c) (Figure 1). Our study is primarily concerned with the spin-up characteristics exhibited by these land surface models (LSMs) for the tropical forest and grassland cases. The lack of complete conservation of energy and moisture does not seem to affect the results presented here.

The spin-up of an LSM is defined as an adjustment process during which the model is approaching its equilibrium. The equilibrium state of a robust LSM should be physically realistic, and its behavior in the adjustment period should be physically meaningful and in accord with real world experience. Two examples are the drying of soil in a severe drought or the wetting of soil during a rainfall event (either thunderstorm or drizzle). Features such as these must be adequately treated by LSMs for use in numerical weather prediction (NWP) models and/or GCMs.

In climate simulations with GCMs, equilibrated climates are usually analyzed. However, the integration time is often restricted by the computing resources. In order to obtain meaningful results, care must be taken when specifying the initial conditions. Soil moisture is one of the variables which is problematic. Global measured data are not available and so the existing global fields of soil moisture have been inferred from simple water budget models containing observed precipitation and surface air temperature as inputs [*Mintz and Walker*, 1993]. Also, soil moisture anomalies affecting surface climate can persist for a long time, as demonstrated from observational investigations [*Namias* 1958, 1963] and numerical studies (see *Mintz* [1984] for a review and *Simmonds and Lynch* [1992] for an update). If the integration time is shorter, the resulting climate is not equilibrated and the results can be misleading. In order to provide some useful insight into the performance of GCM and NWP integrations, we explored some of the primary factors affecting spin-up times and the way in which surface fluxes evolved during the spin-up.

2. Models and Experimental Design

There are 22 models considered in this study (see Table 1a and Table 1b). The forcing data for the first stage of PILPS Phase 1(a) were generated from a simulation using the National Center for Atmospheric Research

Table 1a. List of Participating Land Surface Schemes in PILPS and Their Characteristics of Soil Hydrological Parameterizations for Tropical Forest

Model	Layer Depth, m	Roots	P_{or}	θ_w	K_0	B	Reference
BATS	0.1, 1.5, 10	0.8, 0.2, 0	0.6	0.292	1.6	9.2	*Dickinson et al.* [1993]
BEST	0.1, 1.5	0.8, 0.2	0.6	0.292	1.6	9.2	*Pitman et al.* [1991]
BUCKET (Robock)	1	1-m layer	0.15 m *	—	—	—	*Robock et al.* [1995]
CLASS	0.1, 0.35, 4.10	0.262, 0.395, 0.343	0.6	−150 m †	2.0	9.2	*Verseghy* [1991]
CSIRO	0.01, 1.51	two layers	0.42	0.175	6.3	—	*Kowalczyk et al.* [1991]
GISS	0.1, 0.32, 0.82, 1.94, 4.43, 10	0.80, 0.08, 0.07, 0.05	0.576	−100 m †	1.03	—	*Abramopoulos et al.* [1988]
ISBA	0.01, 1.5	1.5 m	0.477	0.218	1.7	7.75	*Noilhan and Planton* [1989]
TOPLATS	10 m soil column with three zones ‡	1.5 m	0.56	—	1.6	9.17	J. Famiglietti (personal communication, 1993)
LEAF	0.0, 0.1, 0.5, 1.0, 2.0, 4.0, 8.0	1.5 m	0.6	0.291	1.6	9.2	T. J. Lee (personal communication, 1994)
LSX	0.05, 0.15, 0.35, 0.75, 1.75, 4.25	0.1 × canopy height	0.6	0.292	1.6	9.2	D. Pollard (personal communication, 1994)
BUCKET (Man69)	1	1-m layer	0.15 m *	—	—	—	P. C. D. Milly (personal communication, 1993)
BUCKET (PILPS)	1	1.5-m layer	0.225 m *	—	—	—	P. C. D. Milly (personal communication, 1993)
MIT	0.1, 1.4, 8.5	1.4 m	0.6	0.292	1.6	9.2	*Entekhabi and Eagleson* [1989]
MOSAIC	0.1, 1.5, 10	1.5 m	0.6	0.234	1.6	9.2	*Koster, Suarez* [1992]
NMC/MRF	0.15	—	—	—	—	—	H. Pan (personal communication, 1993)
CAPS/OSU	0.05, 1.0	0.05, 0.95	0.435	0.114	34.67	4.9	M. Ek (personal communication, 1993)
PLACE	0.01, 0.1, 1.5, 10, 100	second layer: 0.8; third layer: 0.2; other: 0	0.6	0.144	1.5	9.2	P. Wetzel (personal communication, 1993)
BUCKET (Rstom)	1	1.5-m layer	0.225 m *	—	—	—	P. C. D. Milly (personal communication, 1993)
SECHIBA	two layers	1 m	0.15 m *	?	?	?	*Ducoudre et al.* [1993]
SSiB	0.1, 1.5, 10	top two layers	0.6	0.192	1.6	9.2	*Xue et al.* [1991]
UKMET	0.04, 0.196, 0.758, 2.544 §	1.5 m	0.6	0.292	1.6	9.2	J. Lean (personal communication, 1993)
VIC	1, 10	0.90, 0.10	0.6	0.292	1.6	9.2	X. Liang (personal communication, 1993)

P_{or}, porosity; θ_w, fraction of water content at which permanent wilting occurs; K_0, maximum hydraulic conductivity ($\times 10^{-6} ms^{-1}$); B, Clapp and Hornberger parameter; dash, not applicable; question mark, unknown for this study; and "roots", rooting depth or roots fraction.

*Soil plant-available water-holding capacity.

†Soil water suction.

‡The three zones are root zone, percolation zone, and saturated layer.

§These layers are used in computing soil temperatures only.

(NCAR) CCM1. The data were provided at 30-min intervals for 1 year. The results from two sites, tropical forest (60°W, 3°S) and grassland (0°E, 52°N), were examined. The four basic experiments are shown in Table 2a. The DRY experiment may not be physically realistic since the complete dryness of soil can be realized only when the soil is baked in an oven. Nevertheless, this design can ensure that soil layers in different models hold virtually the same (i.e., zero) absolute soil water contents initially, except for bucket-type models [e.g., *Manabe*, 1969]. A more realistic approach, assuming the initial soil moisture at wilting point, would not ensure the same soil moisture content for different models because of the different soil layer depths that are employed in the different schemes.

For bucket-type models (e.g., those by *Robock et al.*

Table 1b. List of Participating Land Surface Schemes in PILPS and Their Characteristics of Soil Hydrological Parameterizations for Grassland

Model	Layer Depth, m	Roots	P_{or}	θ_w	K_0	B	Reference
BATS	0.1, 1.0, 10	0.8, 0.2, 0	0.51	0.193	4.5	6.8	*Dickinson et al.* [1993]
BEST	0.1, 1.0	0.8, 0.2	0.51	0.193	4.5	6.8	*Pitman et al.* [1991]
BUCKET (Robock)	1	1-m layer	0.15 m *	—	—	—	*Robock et al.* [1995]
CLASS	0.1, 0.35, 4.10	0.273, 0.411, 0.316	0.51	−150 m †	4.8	6.8	*Verseghy* [1991]
CSIRO	0.01, 1.01	two layers	0.42	0.175	6.3	—	*Kowalczyk et al.* [1991]
GISS	0.1, 0.32, 0.82, 1.94, 4.43, 10	0.8, 0.1, 0.08, 0.02, 0, 0	0.537	−100 m †	4.93	—	*Abramopoulos et al.* [1988]
ISBA	0.01, 1.0	1.0 m	0.477	0.218	1.7	7.75	*Noilhan and Planton* [1989]
TOPLATS	10 m soil column with three zones ‡	1.0 m	0.47	—	4.5	6.8	J. Famiglietti (personal communication, 1993)
LEAF	0.0, 0.1, 0.5, 1.0, 2.0, 4.0, 8.0	1.0 m	0.51	0.192	4.5	6.8	T. J. Lee (personal communication, 1994)
LSX	0.05, 0.15, 0.35, 0.75, 1.75, 4.25	0.1 × canopy height	0.51	0.193	4.5	6.8	D. Pollard (personal communication, 1994)
BUCKET (Man69)	1	1-m layer	0.15 m *	—	—	—	P. C. D. Milly (personal communication, 1993)
BUCKET (PILPS)	1	1-m layer	0.15 m *	—	—	—	P. C. D. Milly (personal communication, 1993)
MIT	0.1, 0.9, 9.0	0.9 m	0.51	0.193	4.5	6.8	*Entekhabi and Eagleson* [1989]
MOSAIC	0.1, 1.0, 10	1.0 m	0.51	0.158	4.5	6.8	*Koster, Suarez* [1992]
NMC/MRF	0.15	—	—	—	—	—	H. Pan (personal communication, 1993)
CAPS/OSU	0.05, 1.0	0.05, 0.95	0.477	0.18	1.7	7.75	M. Ek (personal communication, 1993)
PLACE	0.01, 0.1, 1.0, 10, 100	second layer: 0.8; third layer: 0.2; other: 0	0.51	0.144	4.5	6.8	P. Wetzel (personal communication, 1993)
BUCKET (Rstom)	1	1-m layer	0.15 m *	—	—	—	P. C. D. Milly (personal communication, 1993)
SECHIBA	two layers	1 m	0.15 m *	?	?	?	*Ducoudre et al.* [1993]
SSiB	0.2, 0.49, 1.49	top two layers	0.42	0.1344	4.5	6.8	*Xue et al.* [1991]
UKMET	0.05, 0.245, 0.948, 3.180 §	1.0 m	0.51	0.19	4.5	6.8	J. Lean (personal communication, 1993)
VIC	1, 10	1.0, 0.0	0.51	0.193	4.5	6.8	X. Liang (personal communication, 1993)

P_{or}, porosity, θ_w, fraction of water content at which permanent wilting occurs; K_0, maximum hydraulic conductivity ($\times 10^{-6}$ms^{-1}); B, Clapp and Hornberger parameter; dash, not applicable; question mark, unknown for this study; and "roots", rooting depth or roots fraction.

*Soil plant-available water-holding capacity.

†Soil water suction.

‡The three zones are root zone, percolation zone, and saturated layer.

§These layers are used in computing soil temperatures only.

[1995] and P. C. D. Milly [personal communication, 1993] as given in Tables 1a and 1b), the "soil moisture content" does not refer to the absolute soil moisture content. Rather, it represents the "plant-available soil moisture content," W, and $0 \leq W \leq W_f$, where W_f is a bucket field capacity. This terminology was first introduced in climate modeling by *Manabe* [1969] and has been used since. It is, however, often confused with the "field capacity" defined in soil sciences, in which the bucket field capacity, W_f, has long been called "soil plant-available water-holding capacity." W_f is defined as

$$W_f = (\theta_f - \theta_w) D, \quad (1)$$

where D is the total depth of soil layer, θ_w is the volumetric water content at the permanent wilting point, and θ_f is the volumetric water content at field capacity.

Table 2a. List of Experimental Details for PILPS

Experiment	Description
CTRL	All models were initialized for January 1, all soil moisture stores were initialized at 50% of full capacity whether liquid or frozen, the canopy (if present) was initialized at 50% full, snow mass and snow age (if any) were initialized at zero, all soil or canopy temperatures were initialized at 300 K for forest and 275 K for grass. A single year of forcing was repeated exactly every year during integration.
DRY	As in CTRL but all moisture stores were initialized at dry.
WET	As in CTRL but all moisture stores were initialized at full capacity.
NOP	As in CTRL but the simulation was started from the end of the DRY, and precipitation was set to zero throughout.

Since there is only one layer, that is, the root zone, for the bucket-type models, the total depth of soil layer is also the rooting depth. Since the bucket-type models and the nonbucket-type models are so different in concepts, it is difficult to derive W_f for the bucket-type models based on the vegetation and soil characteristics specified for the nonbucket-type models in the PILPS experiments (see Table 3). As shown in Tables 1a and 1b, therefore, *Robock et al.* [1995] use $W_f = 15$ cm for both forest and grassland, while Milly takes $W_f = 22.5$ cm for forest and $W_f = 15$ cm for grass. Initializing W to zero in these bucket-type models does not mean the absolute soil moisture content is zero. Rather, it means that the absolute soil moisture content is at the permanent wilting point. This inconsistency, however, does not alter our conclusions.

In addition to the four experiments described above, the Biosphere-Atmosphere Transfer Scheme (BATS) [*Dickinson et al.*, 1993] was used to carry out additional experiments (Table 2b) to clarify the sensitivities of some model parameters and climate variables. Some of these results have shed light on the differences among the land surface models.

3. Definition of Spin-Up Time

Since a single year of forcing was repeated exactly every year, complete spin-up would have occurred if the model's state at year $n+1$ is identical to that at year n. In practice, however, such perfectly identical states between 2 years cannot always be realized. According to a survey of the notes supplied by each participating group concerning their models' performances (Table 4), there is no consensus regarding the definition of equilibrium and the associated spin-up time and, for most models, as more significant digits are considered, n will increase. However, achieving such a highly accurate equilibrium is unnecessary.

Here the spin-up time is defined as year n, if

Table 2b. Details of Additional Experiments With BATS

Experiment	Description
N	As in CTRL in Table 2a.
V1	As in N but the maximum vegetation cover fraction is set to unity, and the seasonal range is set to zero.
V0	As in N but the maximum vegetation cover fraction and the seasonal range are set to zero.
HFD	As in N but the total depth of the soil active layer was halved.
HFHFD	As in N but the total depth of the soil active layer was reduced to one-fourth of the original.
HFP	As in N but the precipitation intensity was halved.
HHDP	As in HFHFD but the precipitation intensity was halved.
HFS	As in N but the intensity of the incident solar radiation was halved.
DBR	As in N but the stomatal resistance was doubled each time step after calculation.

Table 3. List of Soil Parameters Prescribed in the PILPS Experiments

Soil Parameters	Grass	Forest
Bucket field capacity, m	0.15	0.15
Critical soil moisture, m	0.75×0.15	0.75×0.15
Depth of top soil layer, m	0.1	0.1
Rooting depth, m	1.0	1.5
Total soil depth, m	10.0	10.0
Fraction of total roots in top soil layer	0.80	0.80
Soil porosity	0.51	0.60
Minimum soil suction, m	0.2	0.2
Maximum hydraulic conductivity, m/s	4.5×10^{-6}	1.6×10^{-6}
Permanent wilting point, m^3water/m^3soil	0.378×0.51	0.487×0.60
Clapp and Hornberger "B" parameter	6.8	9.2
Ratio of soil thermal conductivity to that of loam	0.95	0.80

$$|LE^{n+1} - LE^n| < 0.1 \text{ and } |H^{n+1} - H^n| < 0.1, \quad (2)$$

where LE and H are annual mean latent and sensible heat fluxes in Wm^{-2}, respectively. The use of annual mean values will not resolve $n < 1$ year. Also, our constraint of 0.1 Wm^{-2} is less strict than that used in GISS, SSiB, and VIC shown in Table 4 but is still strict enough considering an observational accuracy of around 10 Wm^{-2} [*Leese*, 1993]. Other definitions of spin-up times, such as e-folding time [*Delworth and Manabe*, 1988] or halving time [*Simmonds and Lynch*, 1992], are even less strict than our restraint and produce a smaller n (see section 4.1).

In the case of the zero precipitation runs, there is a less strict condition that both absolute values must be less than 0.5 Wm^{-2}. In rare cases, n has to be determined by plotting LE and H against time in years. From those curves, it is straightforward to determine the spin-up time of a particular model/experiment.

Using the above definition, the results from all the models were processed and a consistent set of spin-up times was obtained. These values give considerably smaller spin-up times than those previously obtained by some groups (Table 4). For example, the spin-up time for the GISS NOP experiment is 49 years against the previous estimate of 268 years for tropical forest and 70 years against 377 years for grassland. These results are described in section 5.

4. Analysis

4.1. Timescale Analysis for Bucket Model

Numerous sensitivity studies [e.g., *Hunt*, 1985; *Simmonds and Lynch*, 1992, and references therein] have demonstrated that the initial water content of the soil plays an important role in the evolution of surface latent and sensible heat fluxes and that this effect has a

Table 4. Definitions of Model Equilibrium and Spin-Up Times by Selective Participating Groups

Model/Group	Description	n (NOP)
PILPS	Results at year n are identical to results at year $n+1$.	
BUCKET (Milly)	For NOP experiments, the latent heat flux is less than 0.01 Wm^{-2}; for other experiments, results at year n are identical to results at year $n+1$.	1
GISS	All the monthly means in the output file (skin temperature, latent heat flux, sensible heat flux, total runoff and snow water equivalent depth) at year $n+1$ are within one part in 10^4 of the corresponding values at year n.	268 (TRF), 377 (GRA)
SSiB	The differences of SSiB's output between years n and $n+1$ are less than 0.1%.	56 (TRF), 41 (GRA)
VIC	The mean, maximum and minimum of each of the land surface fluxes at year n are identical to those at year $n+1$ at the fifth significant digit.	76 (TRF), 53 (GRA)

A general definition adopted in this study is given in the text, and new values of n for NOP are given in Figure 6.

long memory. Therefore it was appropriate to perform a timescale analysis of the soil mositure anomaly before proceeding to a formal discussion of the results from each of the 22 models. A simple case was considered first. The rate equation for bucket-type models is

$$dW/dt = P - E - R, \tag{3}$$

where W is the depth of water (millimeters), P is rainfall input (millimeters per day), E is evaporation (millimeters per day), and R is runoff (millimeters per day). In the bucket model, $P = 0$ implies $R = 0$. In this case, the bucket of water will dry out as a result of evaporation. Thus

$$dW/dt = -E. \tag{4}$$

After an amount of time τ, there is no water left in the bucket. Then,

$$\int_{W_{\max}}^{0} dW = \int_{0}^{\tau} -E\,dt. \tag{5}$$

If E is assumed to be a constant,

$$\tau = W_{\max}/E. \tag{6}$$

If $W_{\max} = 150$ mm and $E = 1$ mm/d, $\tau = 150$ days. If $W_{\max} = 4000$ mm and $E = 1$ mm/d, $\tau = 4000$ days $\approx$ 11 years. Clearly, the time taken to dry up the bucket is proportional to the initial water amount the bucket holds and inversely proportional to the magnitude of evaporation.

Constant E is an extreme case. More realistically, evaporation is assumed to take the form

$$E = \beta E_p, \tag{7}$$

where

$$\beta = \begin{cases} W/(0.75W_f) & \text{if} \quad W < 0.75W_f \\ 1 & \text{if} \quad W \geq 0.75W_f \end{cases} \tag{8}$$

E_p is potential evaporation, and W_f is soil plant-available water-holding capacity as defined in (1). Equations (3), (7) and (8) together define the "bucket model" which was first employed in the Geophysical Fluid Dynamics Laboratory GCM by *Manabe* [1969].

To characterize the stability of soil moisture storage, we seek a τ similar to that in (6). Assuming there is no precipitation and E_p = constant, then the time taken for soil moisture stores to dry up from W_f to $0.75W_f$ is

$$\tau_1 = 0.25W_f/E_p. \tag{9}$$

When $W < 0.75W_f$, substituting (7) and (8) into (4) gives

$$dW/dt = -\lambda W, \tag{10}$$

where λ is a constant given as

$$\lambda = E_p/(0.75W_f). \tag{11}$$

Equation (10) can readily be integrated to give an exponential decline in the soil moisture content W and hence an e-folding time of W is $1/\lambda$. This is also the e-folding time of evaporation. Another useful concept is half time, τ_2, defined as the time at which W decreases from $0.75W_f$ to $0.75W_f/2$ and takes the form

$$\tau_2 = \ln 2/\lambda = 0.693/\lambda. \tag{12}$$

This equation shows the half time is 0.693 times the e-folding time which, combined with (9), is essentially equivalent to (6). All are inversely proportional to potential evaporation and proportional to soil plant-available water-holding capacity. The timescale estimated using these formulae is about 3 times smaller than that from (2). Let us take the tropical forest case and BATS for example. Assuming that W_f = 2000 mm (see Figure 2a) and the annual mean E_p = 120 $\mathrm{Wm}^{-2} \approx 4.15$ mm/d (see Figure 8), then the complete dry out timescale following (6), the e-folding time using (11), and half time using (12) are 482, 362, and 251 days, respectively. The spin-up time determined by (2) is 3 years (Figure 4a). It is important to note that the E_p used in bucket models is not a constant in reality but depends on soil temperature, so tends to increase

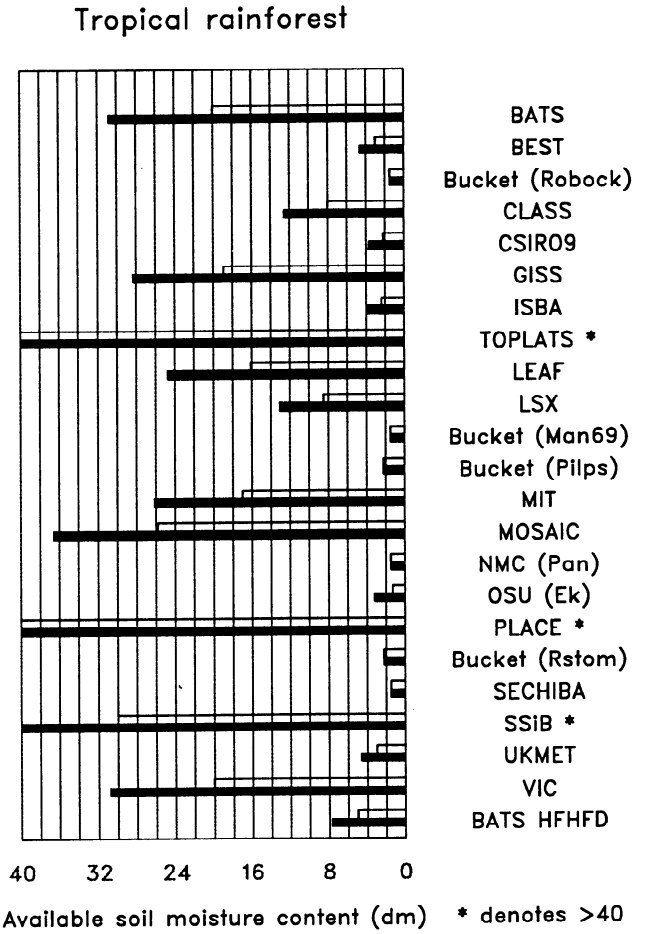

Figure 2a. Maximum available soil moisture content (solid bar) and soil plant-available water-holding capacity (open bar) in the total soil layer for the participating land surface schemes in PILPS for the tropical forest case.

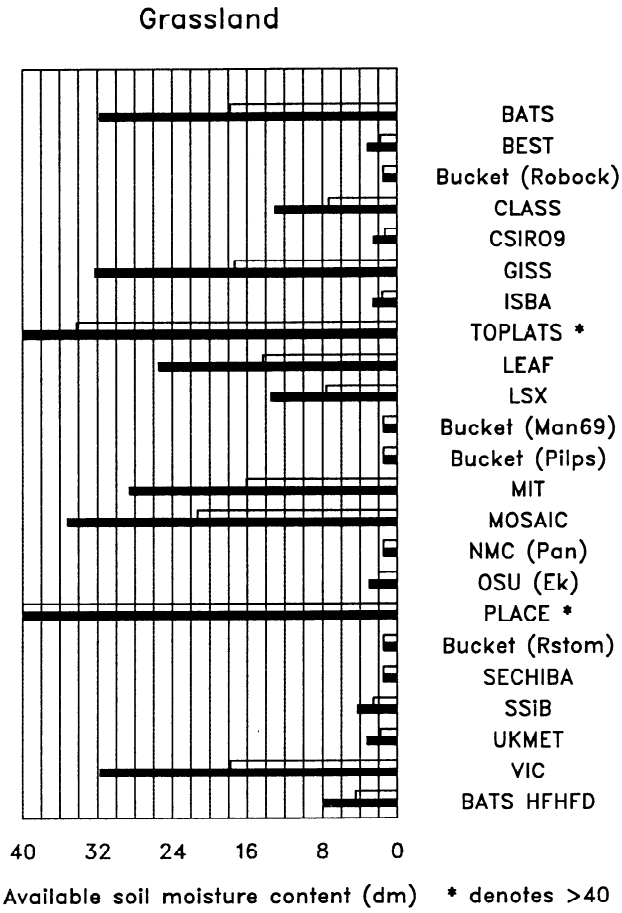

Figure 2b. As in Figure 2a but for grassland.

significantly as the soil dries. Thus (10) no longer gives a simple exponential as a solution.

In deriving (6), (11), and (12), we assumed that precipitation is equal to zero. Alternatively, a timescale can also be derived when there is precipitation. When snowpack is present, the rate equation may be written as

$$\frac{dW}{dt} = -\frac{E_p}{0.75W_f} W + P + S_m - R, \qquad (13)$$

where S_m is snowmelt rate. *Delworth and Manabe* [1988] have pointed out that there is a mathematical resemblance between (13) and a first-order Markov process, which is defined by

$$\frac{dy(t)}{dt} = -\lambda y(t) + z(t), \qquad (14)$$

where λ is a constant and $z(t)$ is a random (white noise) process. Equation (14) is also called "the first-order self-regression equation" [*Huang and Li*, 1984]. The output of the above first-order Markov process is commonly called "red noise" in meteorology. By analogy, the temporal variability of soil moisture in (13) can be approximately regarded as governed by a red noise process if $(P + S_m - R)$ closely resembles white noise. *Delworth and Manabe* [1988] have shown that there is a good agreement between soil moisture (e-folding) decay timescales (defined by $1/\lambda$ and derived by fitting a theoretical red noise spectrum to the model soil moisture spectrum at each grid point) and the evaporative damping timescales (defined as W_f/E_p) in terms of geographical dependence (their Figures 7 and 8b). Therefore in (13) the soil moisture decay timescale is proportional to W_f and inversely proportional to E_p; this is further confirmed by *Milly and Dunne* [1994] using both the bucket model and the GCM similar to those by *Delworth and Manabe* [1988]. However, caution should be taken in understanding this relationship as well as the mathematical resemblance between (13) and (14). First, λ is a constant in (14), but the corresponding factor in (13), $E_p/0.75W_f$ is not a constant, as mentioned above. Next, (13) contains complex feedback processes among W, E_p, P, S_m, and R, but $z(t)$ is, by definition, the external forcing. For example, as W decreases, surface temperature and E_p may increase. This may create a low-pressure system, induce moisture convergence, and increase P. On the other hand, as W decreases, the actual evaporative flux may decrease. This may reduce the local water vapor source to precipitation and decrease P. The conclusion by *Delworth and Manabe* [1988] suggests that these feedbacks may, to a large extent, cancel each other.

4.2. Timescale Analysis for Multiple Soil Layer Model

In the complex models like BATS, PLACE, and MOSAIC (references in Table 1) which explicitly account for vegetation, there are multiple layers and there are different proportions of roots in each layer. Accordingly, the rate equation of soil moisture in each layer is more complicated due to the water transfer between layers and the water uptake by the roots. In BATS [*Dickinson et al.*, 1993], for instance, three soil layers are explicitly included. In the case of tropical forest (Table 1a), the thickness of the three layers was 10 cm for the surface layer, 1.4 m for the subsurface layer, and 8.5 m for the recharge zone. The roots were available only in the top two layers. Assuming that all the soil moisture stores are initially full and that τ_i represents the (e-folding) timescale for the ith layer, a crude analogue to the bucket model leads to the following estimate

$$\tau_i \approx W_{fi}/E_{pi}, \qquad i = 1, 2, 3, \qquad (15a)$$

where W_f is the field capacity and E_p is potential evapotranspiration. In the case of the third layer (recharge zone), E_p is the potential value of water flux at the interface between the second and the third layers. Therefore the e-folding time of total soil moisture can be approximately written as follows

$$\tau \approx \max(\tau_i), \qquad i = 1, 2, 3. \qquad (15b)$$

Since the surface soil layer is 10 cm, W_{f1} as given in (1) is much smaller than the bucket field capacity of 15 cm. As a result, τ_1 is probably smaller than the e-folding time for the bucket model, while τ_2 is likely to be about

the same as the bucket model timescale. Variable τ_3 is the greatest term of the three because W_{f3} is the largest. In other words, the total soil moisture e-folding time is largely dependent on the recharge zone soil moisture e-folding time since the depth of the recharge zone is the largest.

The above analysis is shown only for illustrative purposes. The formal derivation of the e-folding time for soil moisture content or evaporation, however, is difficult for four reasons:

1. The linear relationship between the β function and soil moisture content as given in (8) does not hold for the nonbucket models. A general form of E_p is difficult to obtain for different LSMs.

2. The length of precipitation forcing data is too short (1 year) to perform the statistical analysis.

3. A more rigorous analysis would require a study of the time series of the hydrologic variables, such as water flux at the interface of soil layers and the soil moisture content of each layer. Practically, however, this is constrained by the large amounts of information involved and only results for surface temperature, evaporation, sensible heat flux, snow depth, and runoff were collected for the first round of PILPS experiments.

4. Variable θ_f as used in (1) for computation of W_f was not explicitly given for the PILPS experiments (see Table 3), though it may be estimated following some assumptions (see section 4.3).

As an alternative to the use of W_f, D_w (defined as maximum available soil moisture content, refer to next section for details) is available to estimate water-holding capacity. Therefore it may be feasible only to relate the spin-up time n as defined in section 3 to D_w for the total soil layer. It would then be possible to compare plots of the spin-up time and D_w and to determine the relationship between them, thereby verifying the truth of (15a-15b). Due to the difficulty involved in defining E_p for all the LSMs, we do not attempt in this study to establish an equation between n and E_p.

4.3. Maximum Available Soil Moisture Content

The definition of D_w is as follows

$$\begin{aligned} D_w &= P_{or} D - \theta_w D \\ &= (P_{or} - \theta_w) D , \end{aligned} \tag{16}$$

where D is the depth of the total soil layer, P_{or} is the porosity (m^3m^{-3}), and θ_w is the wilting point (m^3m^{-3}). The relation between D_w and W_f is

$$D_w = W_f + (P_{or} - \theta_f) D . \tag{17}$$

For some types of soil (e.g., clays), θ_f is relatively close to P_{or}, and the difference between D_w and W_f is small, but for sandy soil their difference may be large. In order to illustrate these differences, θ_f is derived for all the nonbucket models by assuming that the drainage by gravity is approximately equal to 2 mm/d and that the Clapp and Hornberger type of drainage formula [*Clapp and Hornberger*, 1978] is used by each model. Thus θ_f takes the following form

$$\theta_f = P_{or}(K_r/K_0)^{1/(2B+3)} , \tag{18}$$

where K is the soil hydraulic conductivity, the subscript 0 denotes the saturated case, $K_r = 2.3 \times 10^{-8}$ m/s $\approx$ 2 mm/d, and B is the Clapp and Hornberger parameter [*Clapp and Hornberger*, 1978]. P_{or}, K_0, and B are all given in Tables 1a and 1b. Hence W_f and D_w can be calculated using (1) and (16), respectively.

In CLASS [*Verseghy*, 1991], the soil water potential is given instead of θ_w. Variable θ_w is therefore obtained using the following relation

$$\psi = \psi_0(\theta_w/P_{or})^{-B} ,$$

where ψ is the soil water potential or soil suction (meters). It is assumed that $\psi_0 = -0.2$ m and plants wilt when $\psi = -150$ m. For the GISS model, a similar derivation was performed, although that model does not use the B parameter [*Abramopoulos et al.*, 1988].

In the PILPS experiments all the models, except the bucket-type previously described, were required to use the same values for surface parameters, including soil porosity, wilting point, and the layer depths (see Table 3). According to our survey (Tables 1a and 1b), almost all of the models used soil porosity and wilting point values as provided. However, most of the models used their own discretization parameters for soil layers while GISS, MOSAIC, SSiB, TOPLATS, and VIC used 10 m total soil depth, as used in BATS. In the following analysis, D_w for the bucket-type models is represented by W_f, as given in Tables 1a and 1b, although by definition they are not the same.

Figure 2a shows D_w and W_f for various models for tropical forest. D_w is greater than 3 m (i.e., 30 dm) for BATS, TOPLATS, MOSAIC, PLACE, SSiB, and VIC, 2.4–2.8 m for GISS, LEAF, and MIT, 1.2 m for CLASS and LSX, and 0.2–0.8 m for the other models. A similar statement (except for SSiB) holds for grassland (Figure 2b). W_f is closer to D_w for tropical forest than for grassland. Since most models use similar values for porosity and wilting point, the differences in D_w or W_f are primarily attributed to the different values of total soil layer depth (Tables 1a and 1b). Conceptually, W_f should be used as a scale factor here because it is the maximum amount of water that can be stored up for evapotranspiration by plants. However, since θ_f was not explicitly given for the PILPS experiments, different nonbucket-type models may have different assumptions than those used in (18) to obtain values of W_f. For instance, the GISS model does not use the Clapp and Hornberger formula. In the following analysis D_w was used instead of W_f, since both lead to essentially similar conclusions.

5. Results

5.1. Spin-Up Times in PILPS Experiments

Figure 3a depicts spin-up times for various models in the tropical forest CTRL run case. TOPLATS, LEAF,

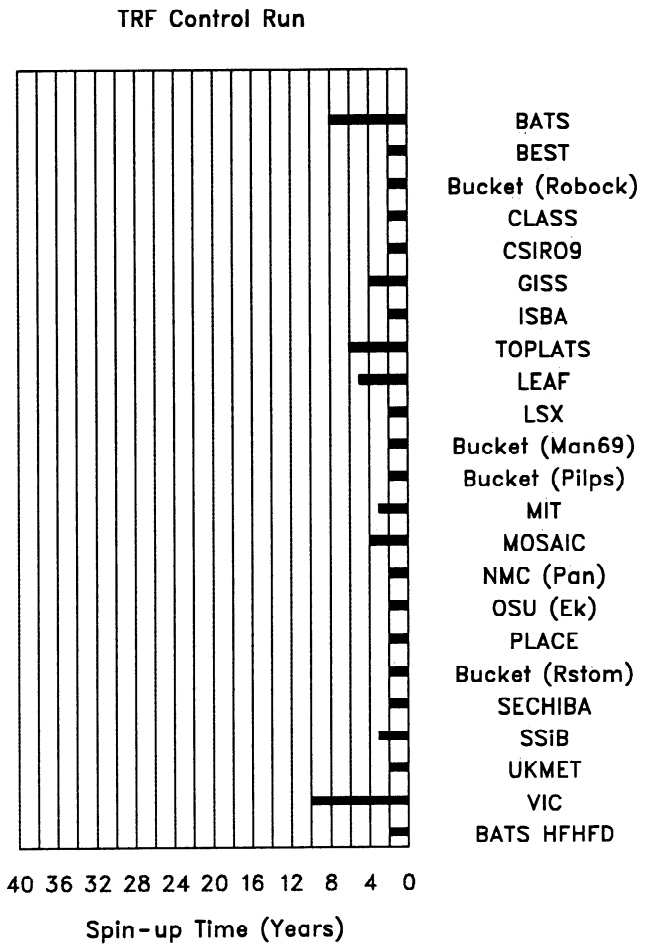

Figure 3a. Spin-up times for CTRL from the participating land surface schemes in PILPS for the tropical forest case.

and VIC did not provide the spin-up data according to the format required by PILPS, so their spin-up time was estimated based on information available in their data. Most models take 2 years to reach equilibrium while VIC needs 10 years, BATS 8 years, TOPLATS 6 years, LEAF, GISS, MOSAIC, SSiB, and MIT all 3–5 years. There is a weak correlation between the spin-up times and the maximum available soil moisture content shown in Figure 2. Roughly speaking, the models with smaller D_w reach equilibrium faster than those with larger D_w. This was anticipated for the bucket-type models based on the simple analysis given in the previous section. In the grassland case (Figure 3b), the basic pattern is similar but the times for VIC, BATS, TOPLATS, and MOSAIC are slightly longer than those for the tropical forest. This longer spin-up time is mainly associated with the weaker intensity of precipitation (compare 1266.0 mm/yr for grassland versus 3267.4 mm/yr for tropical forest), which was also confirmed by a separate sensitivity study with BATS (see section 6).

The spin-up times for WET are shown in Figures 4a (tropical forest) and 4b (grassland). In the case of the tropical forest, BATS, TOPLATS, LEAF, LSX, MOSAIC, and VIC are the models having spin-up times of 5–10 years, compared to 1–2 years for other models. BATS, BEST, CLASS, CSIRO9, GISS, ISBA, TOPLATS, LEAF, MIT, SSiB, and UKMET take a slightly shorter time in WET than in CTRL (compare Figure 3a). This indicates that their initial moisture stores in WET are closer to the equilibrium water stores than those in CTRL (i.e., 50% of capacity). However, LSX and MOSAIC require slightly longer spin-up time in WET than in CTRL, suggesting the initial moisture stores in CTRL are closer to the equilibrium water stores than those in WET. For other models, timescales in terms of years are the same for WET and CTRL. This may be because times less than 1 year are automatically rounded up to 1 year for our analysis. Many similar statements can be made for the grassland case based on comparing Figures 3b and 4b.

The spin-up times for DRY are shown in Figures 5a (tropical forest) and 4b (grassland). BATS, GISS, TOPLATS, LEAF, MIT, MOSAIC, and VIC take 7–25 years to reach equilibrium for tropical forest and 5–31 years for grassland. These timescales are, in general, much longer than those for CTRL. Filling up the soil reservoirs from the dry to the equilibrium level, estimated to be higher than 50% of the models' soil moisture capacity, is a very slow process. Also, SSiB consistently shows a relatively small spin-up time in DRY, WET and CTRL for tropical forest in view of its 10-m-deep soil layer.

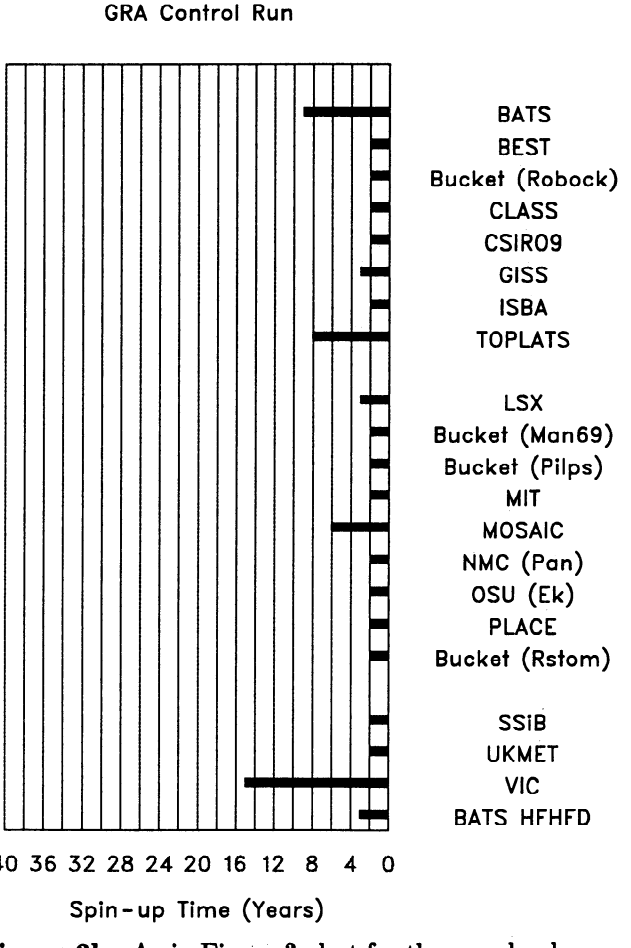

Figure 3b. As in Figure 3a but for the grassland case.

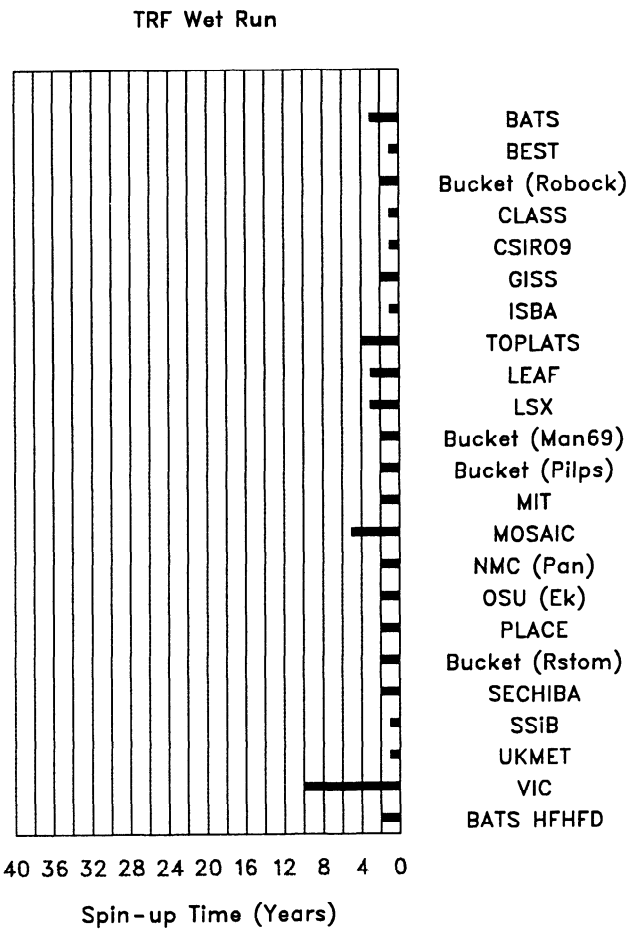

Figure 4a. As in Figure 3a but for WET.

The differences in the spin-up timescales among BATS, GISS, TOPLATS, MOSAIC, VIC, bucket-type models and other models are more pronounced in NOP experiments, as illustrated in Figures 6a and 6b. BATS, GISS, TOPLATS, MOSAIC, PLACE and VIC stand out for both tropical forest (Figure 6a) and grassland (Figure 6b). In the former case, BATS, GISS, MOSAIC, and VIC all take more than 40 years. Comparing Figure 2 with Figure 6a, there is an approximate correlation between the spin-up times for drying out and the maximum available soil moisture content, except for SSiB, in which a rather large D_w corresponds to a very short spin-up time.

Figure 7 presents the maximum available soil moisture content D_w within root zones for various models. The patterns display less scatter than those shown in Figure 2. Most models used about 1–1.5 m of root zone, except VIC and CLASS which assumed that the root zone extended to the bottom of the model soil layer (Tables 1a and 1b). The bucket-type models also assumed approximately 1–1.5 m of root zone. To reiterate, the reasons that D_w is generally smallest for the bucket models are (1) the values shown are actually bucket field capacities [compare W_f and D_w in (17)], and (2) W_f is not properly adjusted to be consistent with that of the nonbucket models [see discussion for (1) in section 2]. Obviously, the maximum available soil moisture within the root zone does not determine the spin-up times since there is soil moisture diffusion between the root zone and the deeper soil layer(s). Nor does it solely control the evapotranspiration (Figure 8). When comparing Figures 7 and 8, a large value for root zone D_w does not necessarily correspond to a high value of evapotranspiration since other aspects may have offsetting effects. These aspects include different parameterizations of resistances, albedos, and surface wetness factors.

In summary, Figure 9a shows the scatter between spin-up time, n, and D_w within the total soil layer for all four forest experiments. A similar graph results from the grassland experiments (Figure 9b). In general, the WET experiments take the least time to reach equilibrium and the CTRL experiments are the next closest. The NOP experiments take the longest time to spin up, while the DRY experiments require a longer time than do the CTRL. For the models with $D_w < 0.9$ m, including all the bucket models and some nonbucket models with very small values of total soil layer, n is less than 4 years for almost all the experiments. There is a rapid increase in n for the DRY and NOP experiments when $1.2 \text{ m} \leq D_w \leq 3.6$ m. A general approximate relationship between n and D_w for all the models and all the experiments may be written as

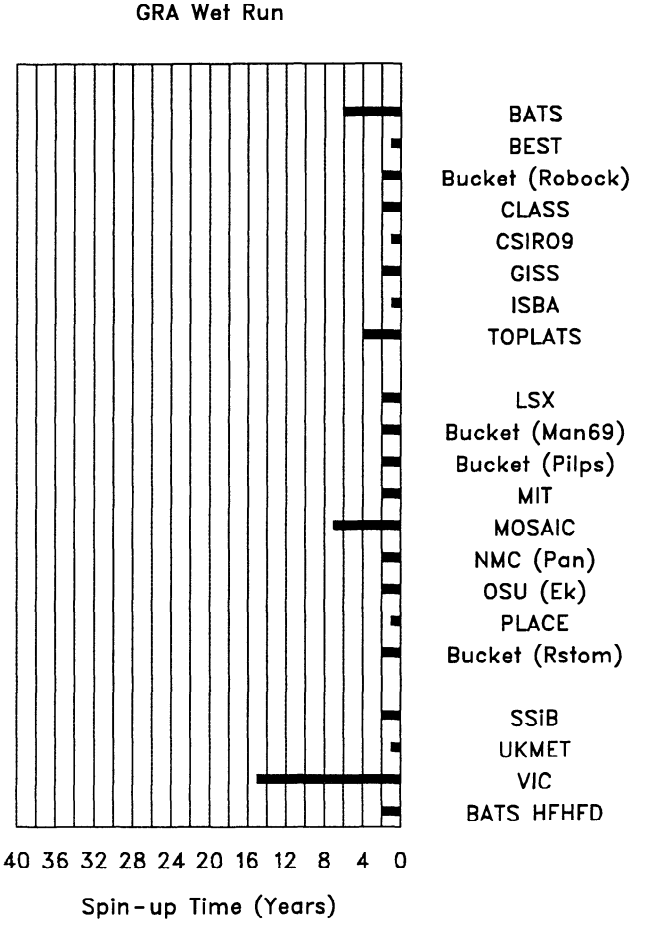

Figure 4b. As in Figure 3b but for WET.

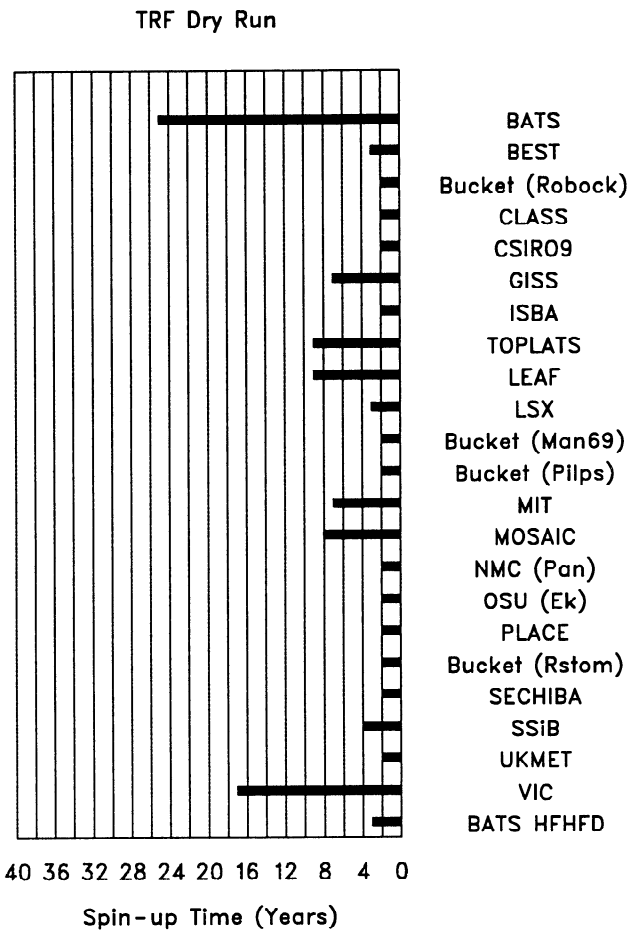

Figure 5a. As in Figure 3a but for DRY.

$$n \approx a\, D_w^b, \tag{19}$$

where a and b are constants, with

$$b_{\mathrm{NOP}} > b_{\mathrm{DRY}} > b_{\mathrm{CTRL}} \geq b_{\mathrm{WET}} \geq 1,$$

where the subscript refers to a particular experiment (NOP, DRY, CTRL, or WET). According to Figure 9, we may write $b_{\mathrm{CTRL}} = b_{\mathrm{WET}} = 1$. This means that the spin-up time varies linearly with the maximum available soil moisture content for CTRL and WET, a conclusion in agreement with that obtained using only the bucket-type models [*Delworth and Manabe*, 1988; *Milly and Dunne*, 1994]. For DRY and NOP, $b > 1$ but $b_{\mathrm{NOP}} > b_{\mathrm{DRY}}$. This means that the spin-up time increases rapidly as D_w becomes large and that the rapidness is greater for NOP than for DRY, a conclusion that can be obtained only through the nonbucket-type models. The reason is that the soil water could be specified (in DRY) or dropped (in NOP) below the permanent wilting point by soil evaporation and drainage, a feature that cannot be realized for the bucket-type models because the available soil moisture (W) cannot be below zero [see (3)]. Since the soil water fluxes (i.e., surface soil evaporation, soil water capillary transfer, and drainage) can be written as a function of soil wetness factor to the power of the B parameter [e.g., *Dickinson et al.*, 1993, pp. 37-39], these fluxes will drop sharply as the soil water amount approaches zero. In this situation, the rate of change of soil water amount becomes very slow. An equation to describe this process may take the following form

$$\frac{dw}{dt} = -k \left(\frac{w}{D}\right)^{B_e}, \tag{20}$$

where w is the absolute soil moisture content, $B_e > 1$ is a linear function of the B parameter, and k is a constant determined by soil characteristics [*Dickinson et al.*, 1993, pp. 37-39]. The term on the right-hand side of (20) denotes the lumped soil water fluxes, which are a nonlinear function of soil moisture content, as opposed to the linear relationship in (10) for the bucket-type models. An integration of (20) leads to the following formula

$$t = c\, D^{B_e}, \tag{21}$$

with

$$c = \left(\frac{1}{(B_e - 1)\, k}\right) \left(w_t^{-B_e+1} - w_0^{-B_e+1}\right).$$

Equation (21) shows that the time (t) taken to dry up the soil water store from w_0 to w_t increases sharply as D increases. This statement is also true when D is replaced by D_w since most of the nonbucket-type models assume the same values of porosity and permanent wilt-

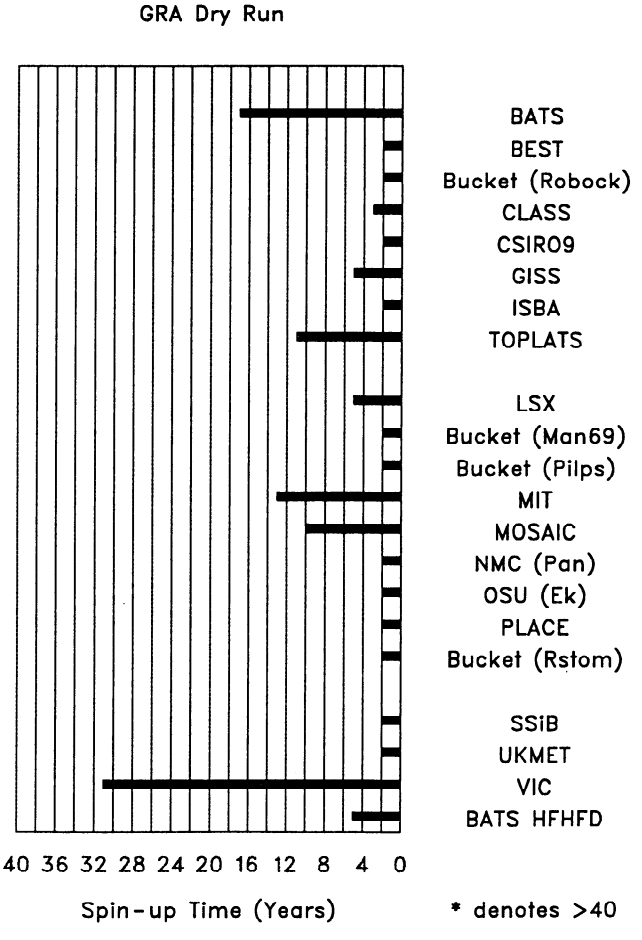

Figure 5b. As in Figure 3b but for DRY.

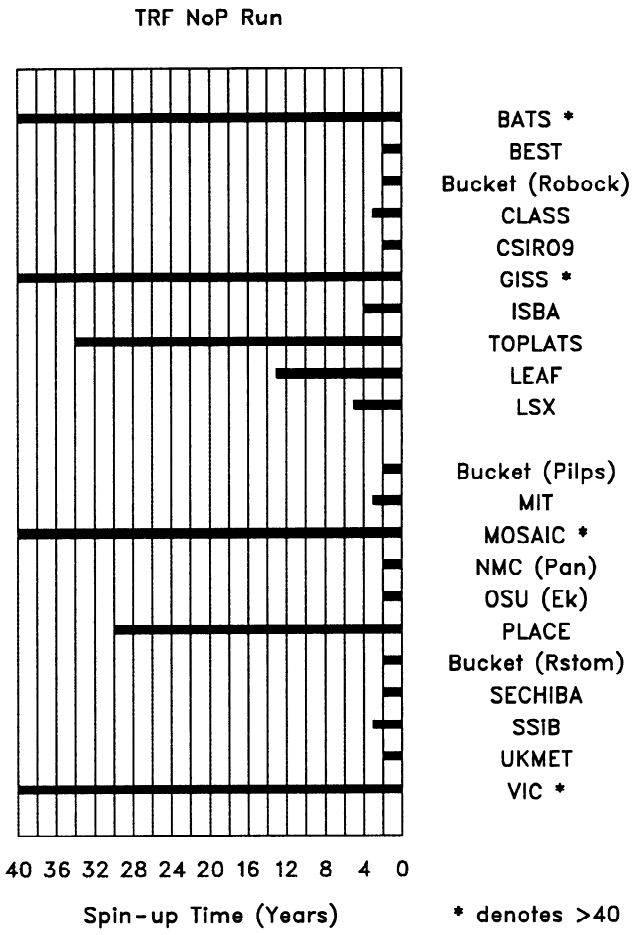

Figure 6a. As in Figure 3a but for NOP.

ing point. Therefore a large D or D_w will drastically increase the evolution time or spin-up time.

However, both TOPLATS and PLACE have large values of D_w but relatively small values of n. TOPLATS is probably the only model which does not include the fraction of water content when wilting occurs. Therefore all the soil moisture in TOPLATS is available for evapotranspiration, which explains why TOPLATS gives the largest value of D_w among the models which used the same values for total soil depth and porosity. This therefore partly accounts for this model's spin-up performance differing from other models. TOPLATS and PLACE appeared to be the only models which contained a saturated bottom layer no matter what the climatic conditions were. Therefore this structure is likely to result in a spin-up path different from the other models. In other words, PLACE and TOPLATS are not compatible with other models as far as the spin-up process is concerned.

The detailed processes in the multilayer LSMs are more complex than those in a simple bucket case as discussed in the previous section. Equation (19) shows that (15) is its special case, a result implying that the multilayer LSMs behave like they have buckets embedded in them and that the temporal variability of soil moisture is likely to be governed by a red noise process. The nonlinear relationship for the DRY and NOP cases suggests that the nonbucket-type models may cover a much wider spectrum of temporal variability than do the bucket-type models.

5.2. Impacts of Soil Moisture Anomalies

All of the participating schemes (but four) have the same equilibria (within accuracy of 0.1 Wm^{-2} for the annual mean latent heat flux) regardless of the initial soil moisture conditions. Among the four diverging schemes, two appear to be still undergoing rapid adjustments, which is consistent with their large values of D_w, and one has the same equilibria for WET and CTRL but they differ by about 1.3 Wm^{-2} from the annual mean value in the last year for DRY. Another scheme has quite large different values of the annual mean latent heat fluxes at year 2, despite its small value of D_w. The three schemes (two with rapid adjustments and one with large different equilibria) are therefore not considered for analysis in this section. In addition, another scheme evidently had problems in properly specifying the initial soil moisture conditions and is thus not considered for the following analysis.

Figure 10 shows the difference of annual mean latent heat fluxes between the CTRL equilibrium and WET at year 1 for the tropical forest. Associated with the initial positive soil moisture anomalies, there are in general

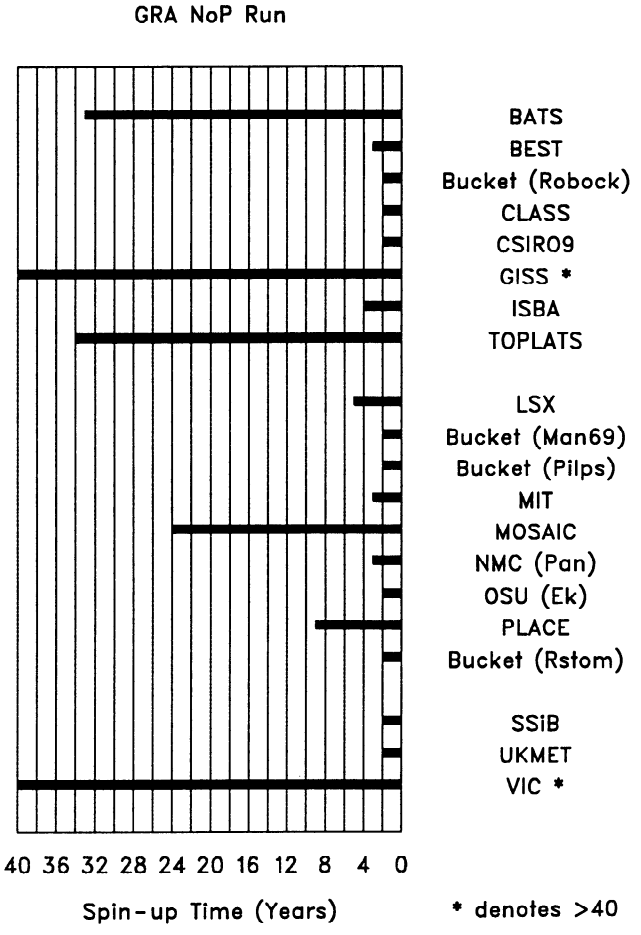

Figure 6b. As in Figure 3b but for NOP.

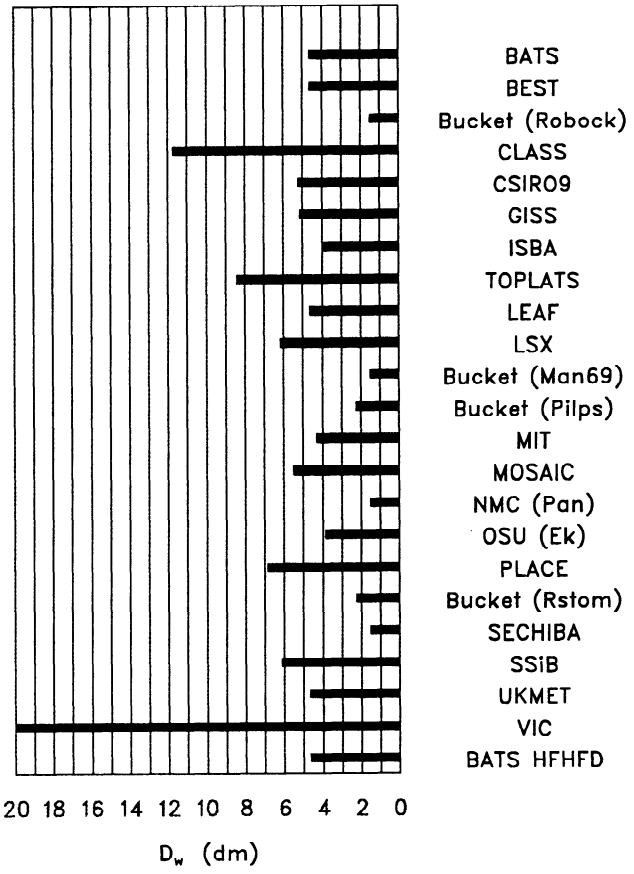

Figure 7. As in Figure 2a but for maximum available soil moisture content in the root zone.

positive anomalies of latent heat fluxes. LSX, Bucket (PILPS), MIT, and MOSAIC stand out, while most of the others show positive, but very small, changes of latent heat flux, implying that use of wet initial conditions is appropriate for these models in the tropical forest. Figure 11 shows the difference in latent heat fluxes between the CTRL equilibrium and DRY at year 1 for the tropical forest. In contrast to the WET case, the initial DRY soil moisture anomalies are accompanied by negative changes in latent heat fluxes. Because these changes are much more pronounced in magnitude, it would likely be better to start with initial conditions too wet than too dry by the same amount. In general, these results show that increasing (decreasing) soil moisture content leads to increases (decreases) of latent heat flux, as expected by intuition and generally found in past modeling studies [see *Mintz*, 1984; *Simmonds and Lynch*, 1992].

6. Results From Additional Experiments With BATS

In order to illustrate the correlation between spin-up times and maximum available soil moisture content more clearly, BATS was used as an example. Figure 12a shows the time evolution of latent heat flux and sensible heat flux from the control (N), WET, and DRY experiments for the grassland case. It can be seen that WET and N converge at about year 7 while DRY displays initial rapid changes toward converging with WET and N but then deviates slowly back to the maximum "divergence" at year 10 before it finally converges at year 17. This behavior in DRY exhibits a unique three-stage feature. At a first glance, the fact that the evaporation for DRY does not monotonically increase from year to year is unexpected. During the first stage (within the first 2 years), the rapid increase in latent heat flux (or decrease in sensible heat flux) implies that the surface atmospheric forcing due to precipitation plays a dominant role and that there is a rapid replenishment in the root zone soil moisture store. During the second stage (from year 2 to year 10), the effects of the diffusion of the root zone soil moisture to the dry recharge zone (i.e., the layer below the root zone) are so predominant that the gradient-driven downward water flow (including the gravitational drainage) can be greater than the net water flux input at the surface. As a result, the root zone soil moisture decreases and hence the evaporation. This stage lasts longer than the first one for two reasons: (1) the magnitude of the downward water flux due to the diffusion is only slightly larger than the net water flux input at the surface, and (2) the thickness of the recharge zone (9 m) is much larger than that of the root zone (1 m). The turning point is the time when the

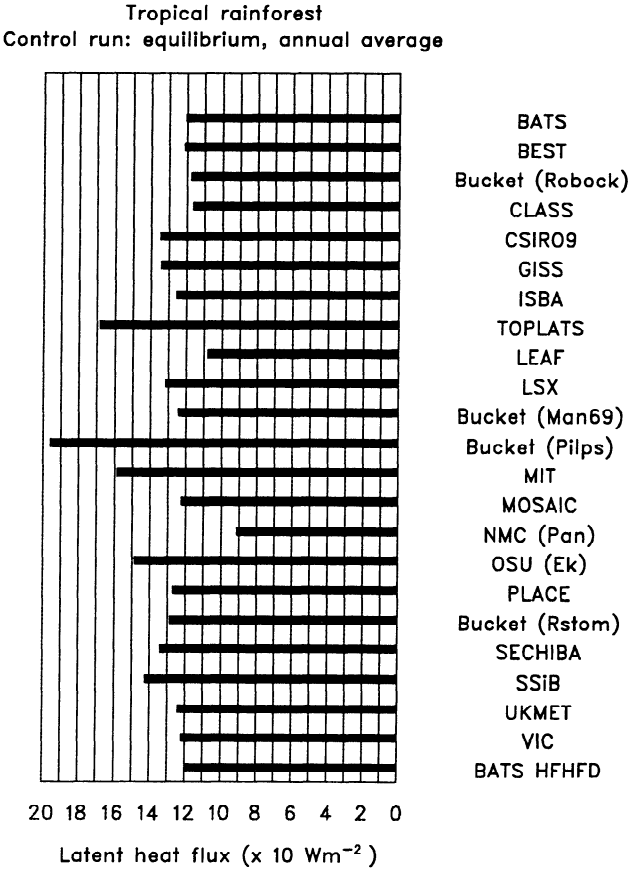

Figure 8. Annually averaged latent heat fluxes at equilibrium for the participating land surface schemes in PILPS: CTRL run tropical forest case.

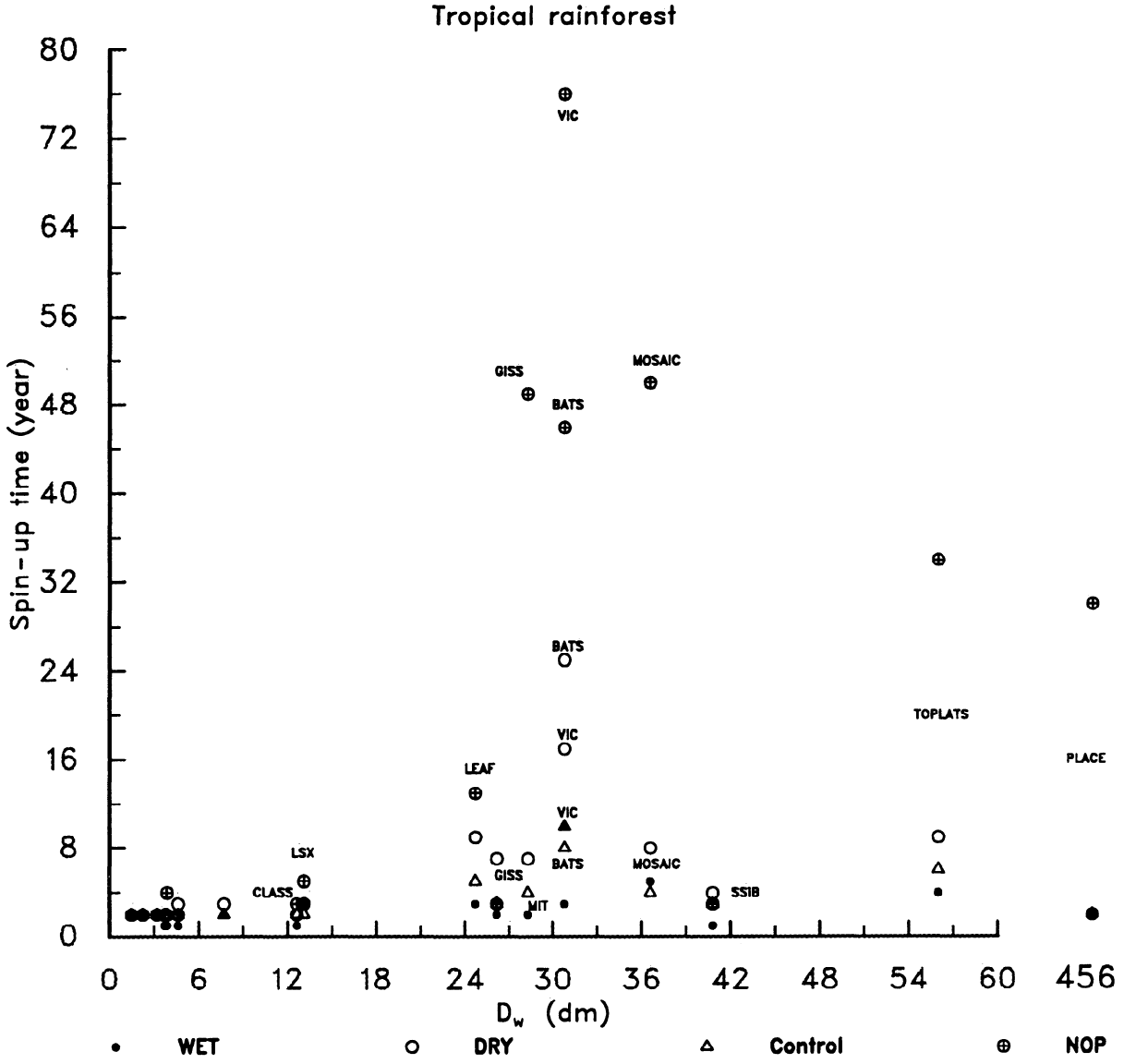

Figure 9a. The scatterplot of the spin-up time (n) and the maximum available soil moisture content (D_w) within the soil layer for the tropical rainforest.

downward water flux due to the diffusion balances the net water flux input at the surface. During the third stage, the slow change in latent heat flux toward converging with WET and N suggests a slow repletion of the recharge zone to the equilibrated state.

Figure 12b shows the time evolution of LE and H from N, WET, and DRY experiments, but all with the total depth being set to one-fourth of 10 m. The three-stage evolution feature in DRY, especially the second stage as illustrated in Figure 12a, does not exist. Therefore the 4-year spin-up period for HFHFD DRY, during which LE displays a monotonous increase, may be a combination of the first stage and a shortened third stage in DRY in Figure 12a.

The significantly long spin-up time in BATS is proportional to the total soil depth under the same meteorological forcings. Figure 13 illustrates that N takes about 8 years to reach equilibrium while HFD (i.e., the total soil depth was halved as defined in Table 2b) takes 4 years. HFHFD (also defined in Table 2b) takes just 2 years when the total depth is set to one-fourth of 10 m. In these experiments the total depth was always greater than the rooting depth. No attempt was made to reduce the total soil depth to a value smaller than the rooting depth. However, it is expected that LE and H will change as well when the total depth is made smaller than the rooting depth.

A summary of spin-up times for various experiments with BATS for tropical forest is presented in Figure 14. The spin-up times for BATS are sensitive to the total soil depth, precipitation intensity and solar radiation, as well as to parameters such as vegetation cover fraction and stomatal resistance. Recall that in the PILPS experiments, all the models used the same atmospheric forcing. In Figure 9a there seem to be factors other than D_w affecting the distribution of points, to some extent. Vegetation cover fraction and stomatal resistance may play a role in this regard.

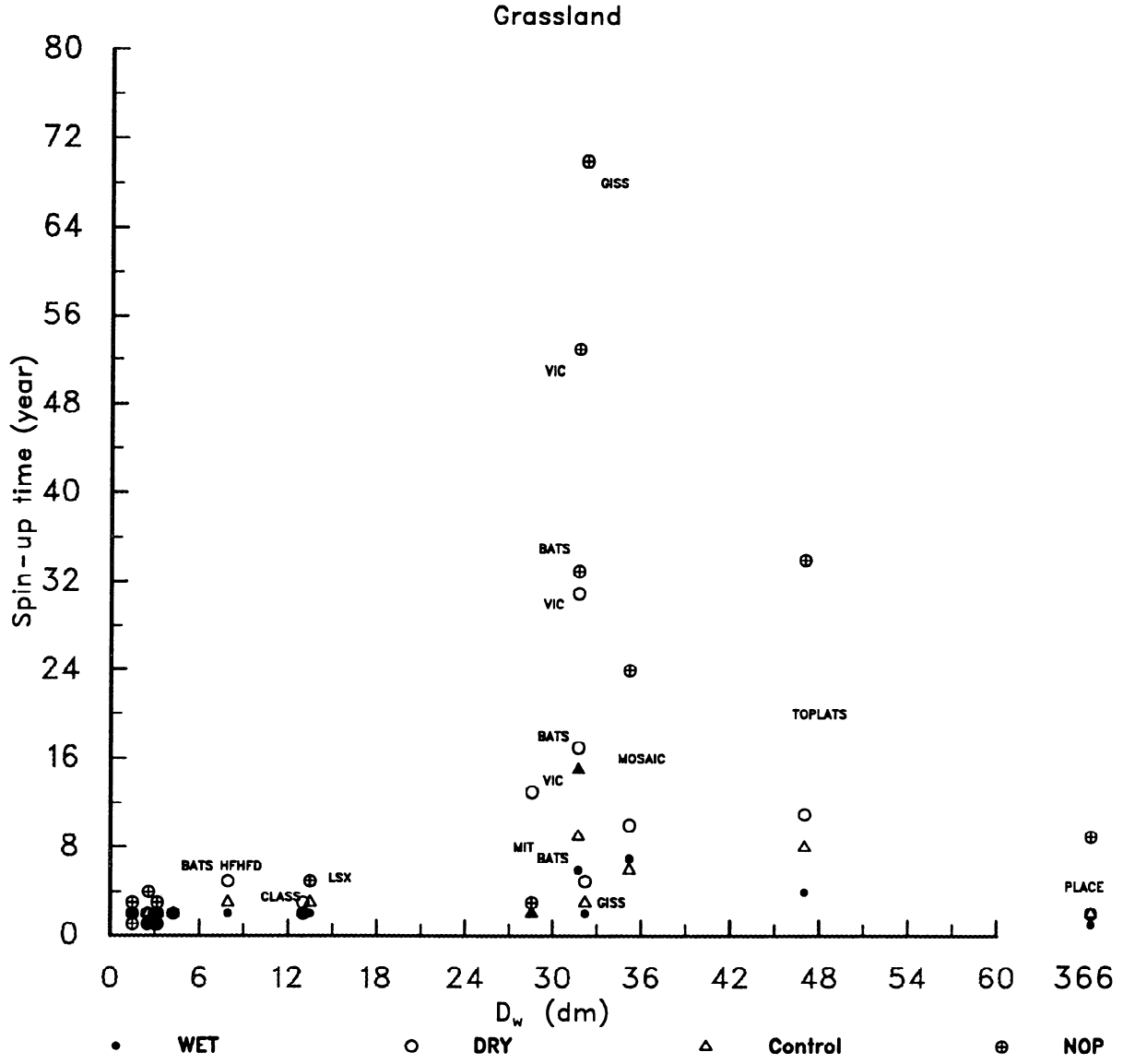

Figure 9b. As in Figure 9a but for grassland.

In light of the demonstrated sensitivity of spin-up time to the total soil depth, it is of interest to see if the simulated heat fluxes exhibit a similar sensitivity. Figure 15 shows the monthly variations of the latent and sensible heat fluxes in the equilibrated year from experiments N, HFD, HFHFD, and HHDP (i.e., the total soil depth was set to 2.5 m and precipitation intensity was halved). There is very little sensitivity of the LE and H to the drastic changes in the total soil depth when it is greater than the rooting depth. In other words, the results show that the equilibrated surface heat fluxes are extremely weakly dependent on the thickness of soil layer below the root zone, despite the strong relationship between spin-up time and this thickness. Presumably for the case examined, the water storage under equilibrated conditions remains sufficient for E and runoff to be unaffected in the wet seasons (i.e., October–April) [see *Pitman et al.*, 1993, Figure 1a]. The small (about -1.0%) but visible changes in LE are in the dry seasons (i.e., May–September). This result indicates that the root zone soil water store is slightly short of supply in the dry seasons and needs to be replenished from the recharge zone. Decreasing the thickness of the recharge zone means reducing the soil water resource for the root zone, though its effect is small. Therefore the decreases in LE from N to HFHFD are slightly larger than those from N to HFD (Figure 15). The annual mean change from N to HFD is about -0.3% for tropical forest (Table 5a), but about -1.2% for grassland (Table 5b or Figure 13) because of the longer dry season [see *Pitman et al.*, 1993, Figure 2b]. As a contrast, when precipitation intensity is halved, LE is reduced by up to 50 Wm^{-2} as shown by the HHDP curve (Figure 15).

The results of the water budgets in these experiments are shown in Table 5. The annual mean or accumulated fields of precipitation (P), evapotranspiration (E) and its components, surface runoff (R_{SUR}), total runoff (R), and soil moisture contents in different soil layers have been tabulated in Table 5. The effective surface tem-

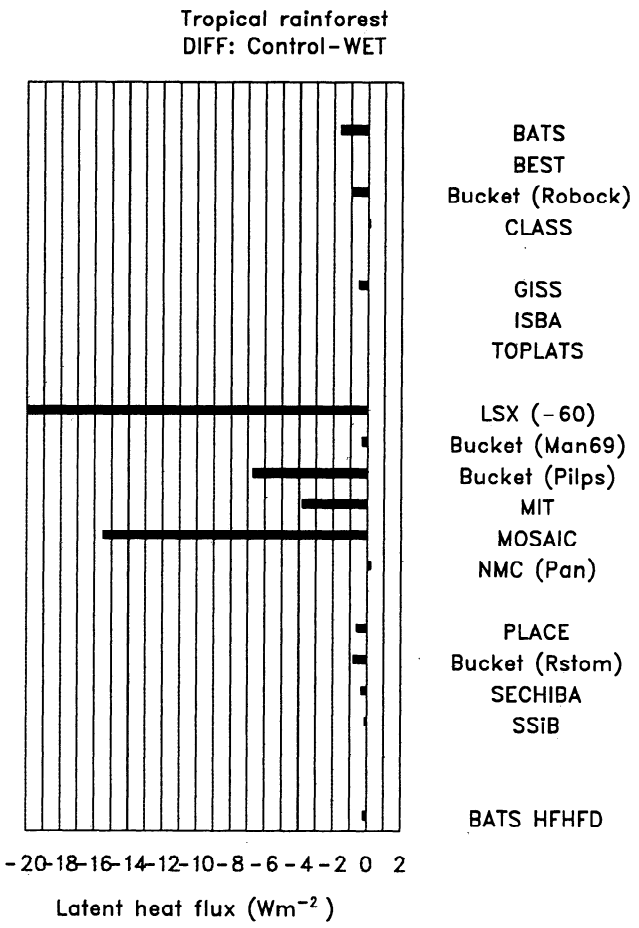

Figure 10. Difference, CTRL – WET, of latent heat fluxes for tropical forest. The values for CTRL are taken from the equilibrium year, while the values for WET are from the first year. In both cases, the annual mean values are used.

perature (T_E) is also included since it is an important variable in both climate modeling and remote sensing. The results are compiled separately for tropical forest (Table 5a) and grassland (Table 5b). Although only BATS has been tested, the conclusions are applicable to many other advanced land surface models.

Overall, BATS reasonably conserves water. The absolute values of $(P-E-R)$ are less than 0.6 mm/yr for tropical forest and about 1–2 mm/yr for grassland. Exceptions are in NOP experiments in which root zone and deeper soil moistures are still adjusting and therefore there is slight transpiration from the root zone. Even in this case, the annual balances are at worst around 5 mm/yr. Since precipitation is prescribed, an increase in E will lead to a decrease by about the same amount in R, and vice versa.

DBR (definition in Table 2b) experiments are designed to assess the responses of surface hydrologic budgets to changes in stomatal resistance. Observations show that in most herbaceous plants, atmospheric CO_2 enrichment tends to significantly reduce the apertures of the leaf's stomatal pores. This effect tends to increase stomatal resistance [*Idso and Kimball*, 1993]. In contrast, in sour orange trees as in many other woody species, CO_2-induced stomatal closure appears to be minimal [*Idso and Kimball*, 1993]. Nevertheless, we considered experiments in which the stomatal resistance was doubled for both tropical forest and grassland. The results are shown in Table 5. The responses are markedly different for both surface types, −13.7% in E for tropical forest and −2.1% for grassland, or different by a factor of 6 to 7. As a result, there are larger increases in soil moisture contents for tropical forest than for grassland.

All the resistance formulations, as given in (A8)–(A12) (see appendix) include the A_v term, while r_s and r_b also include the LAI term. Since both A_v and LAI are prescribed, as in BATS, as quadratic functions of deep soil temperature with its optimum value at 298 K, they are subject to seasonal variation. For tropical forest, this variation is negligible. Hence the maximum vegetation cover (0.9) and maximum LAI (6) were used throughout the year. For the temperate grassland considered in this study, the seasonal variation is so significant that A_v changes from 0.8 in summer to 0.1 in winter, and LAI varies from 2 in summer to 0.5 in winter. Therefore r_s is comparable for tropical forest and grassland in summer (July) as shown in Table 6. Variable r_s

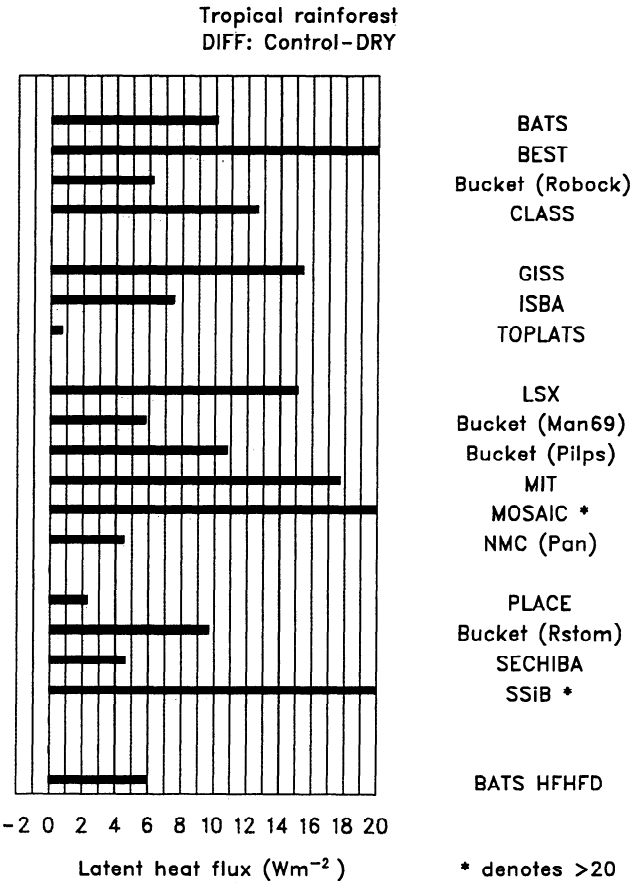

Figure 11. Difference, CTRL – DRY, of latent heat fluxes for tropical forest. The values for CTRL are taken from the equilibrium year, while the values for DRY are from the first year. In both cases, the annual mean values are used.

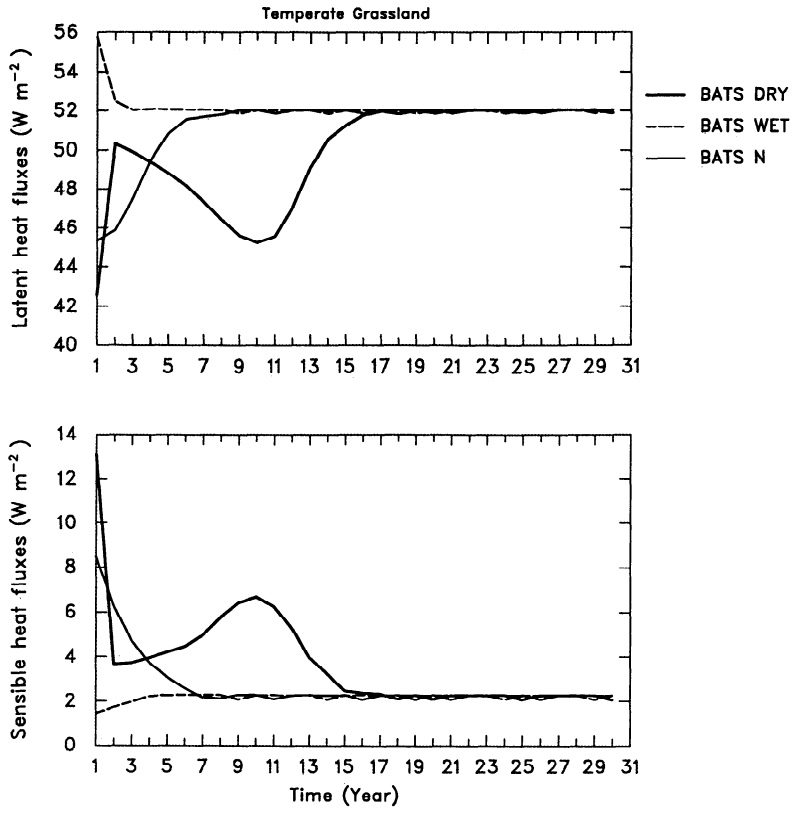

Figure 12a. The evolution of BATS simulated latent and sensible heat fluxes against time (year) for grassland. Refer to Table 2b and text for definitions of experiments. Results from the standard total soil depth given in PILPS (Table 3).

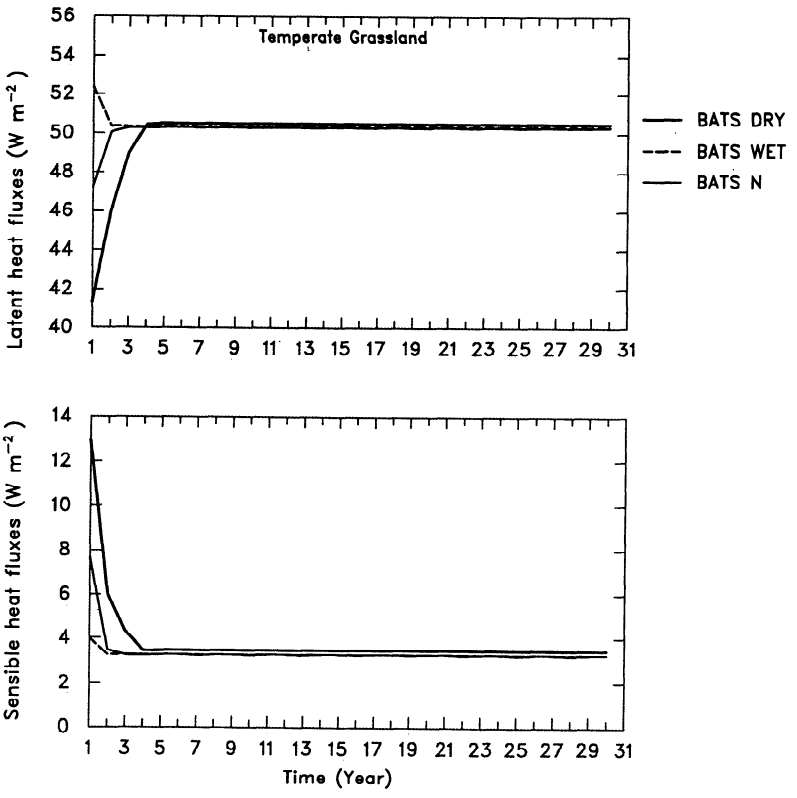

Figure 12b. As in Figure 12a. Results from one-fourth of the standard total soil depth.

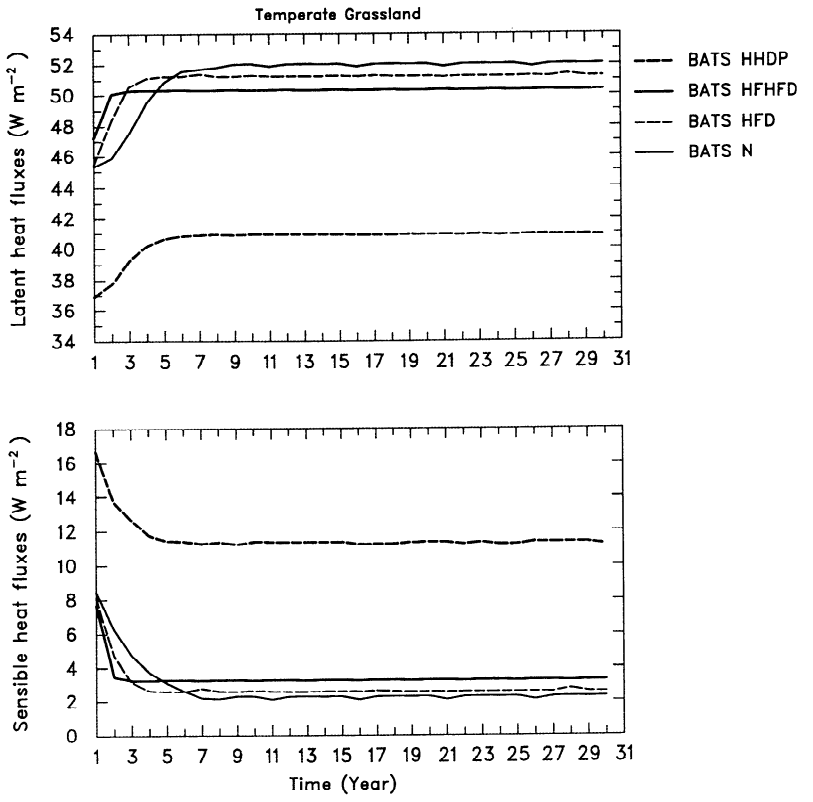

Figure 13. The evolution of BATS simulated latent and sensible heat fluxes against time (year) for grassland. Refer to Table 2b for definitions of symbols.

for grassland becomes very large in other seasons, particularly in January, which is further complicated by the presence of snow cover. Overall, there are greater seasonal variations of aerodynamic and stomatal resistances in grassland than in tropical forest (Table 6).

The different responses in tropical forest and grassland due to doubling of stomatal resistance result from two differences in their resistance to water flux. First, there is the generally recognized difference between aerodynamic resistances, such that in a forest it is an order of magnitude smaller than canopy resistance, while for the grassland they are comparable. Furthermore, the difference is due to the fact that in tropical forest evapotranspiration from the vegetated area (i.e., $E_{TR} + E_{DEW} + E_{UA}$) dominates over evaporation from the bare soil (E_B) (Table 5a), while in grassland the opposite is true (Table 5b). In N, for instance, the annual accumulated evapotranspiration from the vegetated portion is 88% of E for forest and 39% of E for grassland, explaining about half the discrepancy. Primarily, this is because of the relative magnitude of r_a and r_g as shown in Figure 16 and Table 6.

In N, for tropical forest, r_g is greater than r_a by a factor of 30–50, while for grassland, r_g is about equal to or smaller than r_a by a factor of 2–10, except in the midsummer season (Table 6). These differences are traced back further to differences in seasonal vegetation cover fraction. In summer (July), A_v is at maximum for both tropical forest and grassland so that r_g is similar. In other seasons, decreasing A_v in grassland results in decreasing r_g and consequently it becomes smaller than, or comparable to, r_a.

The above results are primarily based on the way in which both A_v and LAI are parameterized in BATS. If they were also functions of soil moisture such that plants also would assume a maximum growth under optimum soil water conditions, the large seasonal variations in A_v and LAI, and then in aerodynamic and stomatal resistance might be reduced. For example, r_s on April 15 for grassland (Table 6) could be much smaller since adequate soil water is available due to snowmelt. Further studies need to be carried out to evaluate these parameterizations against the field data. Both the larger value of r_g and the smaller value of r_a in a tropical forest greatly increase the importance of stomatal resistance for E.

Experiments V1 (maximum vegetation cover fraction set to unity) and V0 (maximum vegetation cover fraction set to zero) also show different results for tropical forest and grassland. For tropical forest, V0 has larger effects than V1: a 14.3% decrease against a 1.7% increase in E. For grassland, V1 has larger effects than V0: a 31.9% decrease against a 4.2% increase in E. For both surfaces, V1 leads to increases in surface soil moisture contents (S_{SW}) and V0 results in decreases in S_{SW}. Changes of soil moisture in the root zone (R_{SW}) due to vegetation cover change are, however, surface dependent.

HFD has negligible effects on S_{SW}, R_{SW}, E and R, though it influences the spin-up time as discussed ear-

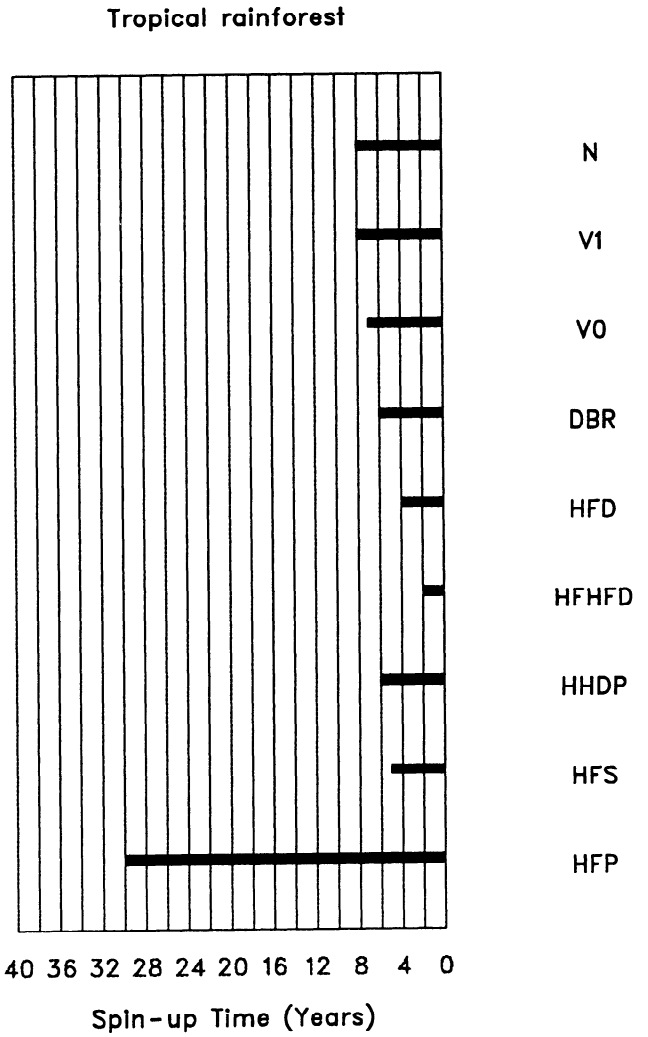

Figure 14. The spin-up times for various experiments with BATS for tropical forest.

lier in this section. HFP leads to a systematically large reduction in E, R_{SUR}, and R. Consequently, it will take a much longer time for BATS to reach equilibrium. All soil moisture stores for both surface types show decreases. In grassland, snow water equivalent (S_{WE}) also decreases. This emphasizes that the accurate prediction of precipitation is one of the most important preconditions for a realistic simulation of soil moisture content in GCMs.

The sensitivities are even more dramatic in NOP, in which R_{SUR} and R are almost zero, E is about 6 mm/yr for tropical forest and 2 mm/yr for grassland, while soil moisture stores are reduced by just 30–60% from their equilibrium values. For tropical forest, the soil moistures at wilting point can be estimated from Table 1a as 29.2 mm, 292.2 mm, and 2922.0 mm. From Table 5 the actual soil moistures for NOP are 16.7 mm, 438.5 mm, and 3344.3 mm. Actual soil moisture content in the surface soil layer has dropped below the wilting point through soil evaporation while transpiration ceases. There is a smaller decrease in R_{SW} and an even smaller decrease in T_{SW}. This is because soil water diffusion between layers in the drying episode becomes weaker. It can be estimated that the complete drying of the surface soil layer may take thousands of years, while the complete drying of the root zone and the total soil layer may not be possible when E and R are equal to essentially zero.

HFS leads to a significantly large reduction in E (−30.8% in tropical forest and −51.2% in grassland) as would be expected since the control of solar radiation, among other elements, on surface evaporation has long been realized and is a basis of the evaporation models proposed by *Penman* [1948] and *Priestley and Taylor* [1972]. There are compensating increases in R (+26.6% in tropical forest and +51.5% in grassland). Both changes in E and R have contradictory effects on spin-up time. As shown in Figure 14, there is a decrease in spin-up time for HFS. To explain this, let A denote the state of climate in N, and B the state of climate in HFS. When solar radiation is halved from state A to state B, relatively speaking, precipitation becomes too high for state B. It is known that spin-up time increases when precipitation is halved; conversely, increasing precipitation decreases spin-up time. Therefore, spin-up time will decrease when solar radiation decreases. As a result of reduction in E, there are increases in soil moisture content in all layers. Conversely, when solar radiation is doubled, there should be decreased soil moisture stores. Hence accurate calculation of solar radiation incident at the Earth's surface is important for a realistic simulation of soil moisture stores in GCMs, that is, cloud amount, type, and optical properties must be correctly simulated.

7. Specification of Total Soil Depth

In the present comparison, most models have used the same values of porosity and wilting point. The differences among the maximum available soil moisture contents are mainly attributed to the different specifications of soil layers. They vary greatly but in general have a root zone and lower zone. Since most of the models assume that the same porosity values apply over the depth of the soil profile, the thicker the model soil, the more water it can hold. The specification of the total model soil depth appears to be an important issue. In short-range numerical weather forecasting studies, the total soil depth may be specified as a rooting depth since the influences of the soil moisture content below the root zone on near-surface weather are negligible; if it is greater than the rooting depth, the spin-up time increases. In climate studies, an arbitrary value of total soil layer depth is used in most LSMs. If this arbitrary value is too large, and is uniformly applied to global land points, a much longer integration is likely to be needed for model climate in middle and high latitudes to reach equilibrium. In other words, if the simulated climate in the tropics has just reached steady state, the results for middle and high latitudes may still be far from being equilibrated, because decreasing solar flux with increasing latitude leads to a long spin-up time (see section 6).

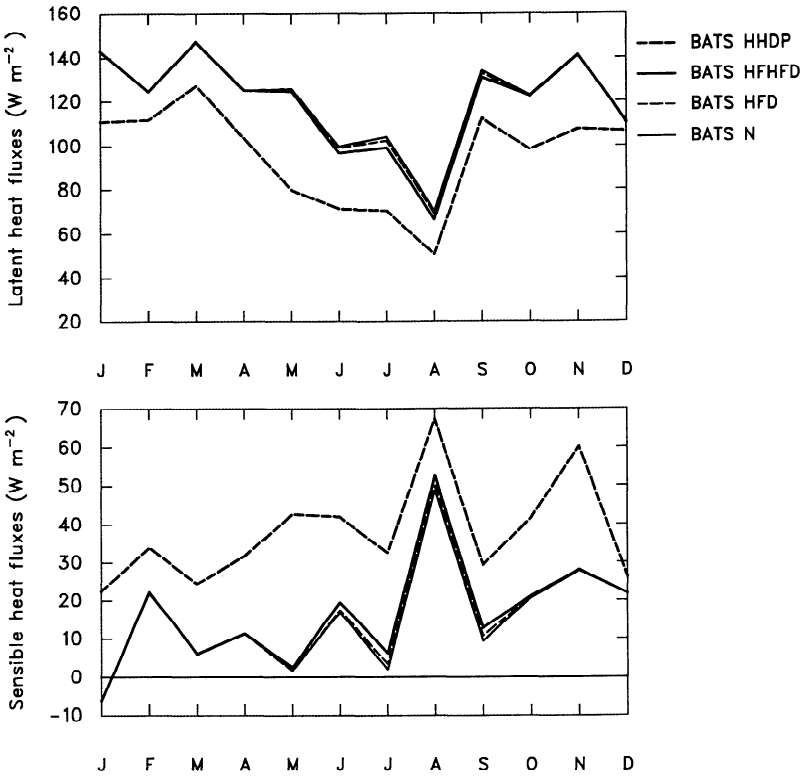

Figure 15. The monthly variation of latent and sensible heat fluxes for various BATS runs for tropical forest. Refer to Table 2b for definitions of symbols.

Table 5a. Annual Mean or Accumulated Fields at Equilibrium for Tropical Forest From Experiments With BATS

	N	V1	V0	HFP	NOP	HFS	HFD	DBR
P	3267.4	3267.4	3267.4	1633.7	0.0	3267.4	3267.4	3267.4
E	1522.4	1548.3	1304.6	1209.6	5.7	1052.8	1517.4	1313.8
	0.0%	1.7%	−14.3%	−20.5%	−99.6%	−30.8%	−0.3%	−13.7%
E_{TR}	640.9	734.0	0.0	512.0	5.0	452.5	639.0	383.9
	0.0%	14.5%	−100.0%	−20.1%	−99.2%	−29.4%	−0.3%	−40.1%
E_{DEW}	527.6	595.4	0.0	445.6	−2.2	375.9	528.2	526.8
	0.0%	12.9%	−100.0%	−15.5%	−100.4%	−28.8%	0.1%	−0.2%
E_{UA}	165.7	218.9	0.0	118.5	1.4	125.1	163.9	186.4
	0.0%	32.1%	−100.0%	−28.5%	−99.2%	−24.5%	−1.1%	12.5%
E_B	188.2	0.0	1304.6	133.5	1.5	99.3	186.3	216.7
	0.0%	−100.0%	593.2%	−29.1%	−99.2%	−47.2%	−1.0%	15.1%
R_{SUR}	1481.5	1469.2	1553.7	421.4	0.0	1692.7	1469.9	1555.0
	0.0%	−0.8%	4.9%	−71.6%	−100.0%	14.3%	−0.8%	5.0%
R	1752.2	1725.9	1969.3	430.7	0.1	2218.2	1757.3	1959.4
	0.0%	−1.5%	12.4%	−75.4%	−100.0%	26.6%	0.3%	11.8%
S_{SW}	38.1	38.7	35.3	32.2	16.7	43.6	38.1	40.9
	0.0%	1.6%	−7.3%	−15.5%	−56.2%	14.4%	0.0%	7.3%
R_{SW}	707.3	704.6	725.6	609.7	438.5	729.4	702.5	721.2
	0.0%	−0.4%	2.6%	−13.8%	−38.0%	3.1%	−0.7%	2.0%
T_{SW}	4997.9	4984.7	5104.9	4276.5	3344.3	5153.9	2484.5	5092.1
	0.0%	−0.3%	2.1%	−14.4%	−33.1%	3.1%	−50.3%	1.9%
T_E	299.8	299.8	299.7	300.1	301.2	299.0	299.8	299.9
	0.0	0.0	−0.1	0.3	1.4	−0.8	0.0	0.1

P, precipitation, millimeters per year; E, total evapotranspiration, millimeters per year; E_{TR}, transpiration, millimeters per year; E_{DEW}, interception loss, millimeters per year; E_{UA}, evaporation from soil below canopy, millimeters per year; E_B, evaporation from bare soil, millimeters per year; R_{SUR}, surface runoff, millimeters per year; R, total runoff, millimeters per year; S_{SW}, soil moisture content in the surface layer, millimeters; R_{SW}, soil moisture content in the root zone, millimeters; T_{SW}, soil moisture content in the total soil active layer, millimeters; and T_E, effective surface temperature, Kelvin. P is prescribed, while all other variables are simulated. The changes relative to experiment N are also included in percentage or difference of temperature.

Table 5b. Annual Mean or Accumulated Fields at Equilibrium for Grassland From Experiments With BATS

	N	V1	V0	HFP	NOP	HFS	HFD	DBR
P	1266.0	1266.0	1266.0	633.0	0.0	1266.0	1266.0	1266.0
E	654.5	445.5	682.1	515.0	2.4	319.2	646.3	640.8
	0.0%	−31.9%	4.2%	−21.3%	−99.6%	−51.2%	−1.3%	−2.1%
E_{TR}	43.5	60.6	0.0	49.6	4.2	22.7	43.8	22.5
	0.0%	39.3%	−100.0%	14.0%	−90.3%	−47.8%	0.7%	−48.3%
E_{DEW}	176.6	275.7	0.0	147.8	−0.3	96.2	176.8	176.5
	0.0%	56.1%	−100.0%	−16.3%	−100.2%	−45.5%	0.1%	−0.1%
E_{UA}	32.6	96.4	0.0	25.5	0.8	22.2	31.6	34.2
	0.0%	195.7%	−100.0%	−21.8%	−97.5%	−31.9%	−3.1%	4.9%
E_B	401.8	12.8	682.1	292.1	−2.3	178.1	394.1	407.6
	0.0%	−96.8%	69.8%	−27.3%	−100.6%	−55.7%	−1.9%	1.4%
R_{SUR}	394.0	426.1	393.1	107.7	2.3	503.6	389.8	393.4
	0.0%	8.1%	−0.2%	−72.7%	−99.4%	27.8%	−1.1%	−0.2%
R	626.8	826.4	598.6	128.5	2.3	949.8	634.1	639.7
	0.0%	31.8%	−4.5%	−79.5%	−99.6%	51.5%	1.2%	2.1%
S_{WE}	3.6	8.1	3.6	1.1	0.0	8.6	3.5	3.5
	0.0%	125.0%	0.0%	−69.4%	−100.0%	138.9%	−2.8%	−2.8%
S_{SW}	32.3	39.3	31.0	24.5	13.3	38.7	32.3	32.4
	0.0%	21.7%	−4.0%	−24.1%	−58.8%	19.8%	0.0%	0.3%
R_{SW}	367.7	377.3	366.0	329.3	194.6	378.5	366.3	368.7
	0.0%	2.6%	−0.5%	−10.4%	−47.1%	2.9%	−0.4%	0.3%
T_{SW}	3998.2	4132.7	3969.7	3464.9	2256.4	4157.5	1989.3	4011.7
	0.0%	3.4%	−0.7%	−13.3%	−43.6%	4.0%	−50.2%	0.3%
T_E	281.3	281.6	281.3	281.8	283.0	279.3	281.3	281.3
	0.0	0.3	0.0	0.5	1.7	−2.0	0.0	0.0

P, precipitation, millimeters per year; E, total evapotranspiration, millimeters per year; E_{TR}, transpiration, millimeters per year; E_{DEW}, interception loss, millimeters per year; E_{UA}, evaporation from soil below canopy, millimeters per year; E_B, evaporation from bare soil, millimeters per year; R_{SUR}, surface runoff, millimeters per year; R, total runoff, millimeters per year; S_{SW}, soil moisture content in the surface layer, millimeters; R_{SW}, soil moisture content in the root zone, millimeters; T_{SW}, soil moisture content in the total soil active layer, millimeters; T_E, effective surface temperature, Kelvin, and S_{WE}, snow water equivalent, millimeters. P is prescribed, while all other variables are simulated. The changes relative to experiment N are also included in percentage or difference of temperature.

The specification of total soil depth is especially important when GCMs are used to study the interannual variability of present-day climate, and transient and doubled climate changes. By utilizing the Palmer drought severity index (PDSI) [*Palmer*, 1965; *Alley*, 1984] and a "supply-demand" drought index, *Rind et al.* [1990] predict that severe drought (5% frequency today) will occur about 50% of the time by the 2050s if greenhouse gas emissions continue to increase rapidly. They also suggest that drought intensification has been understated in most GCM simulations because of their lack of realistic land surface models. Modern LSMs, despite their rapid improvement in the past decade or so, show a wide range of spin-up timescales in the NOP experiments (Figures 6 and 9) and a wide range of heat fluxes in the DRY experiments (Figure 11). The NOP and DRY experiments are the ones which, to some extent, resemble the drought anomalies, and the spin-up times may be understood as related to the periods of low-frequency variability. It can be argued that when these LSMs are linked to a GCM for climate change projections, the drought frequency defined by the model statistics and even the PDSI [see *Rind et al.*, 1990] could be very different for different LSMs.

The range of spin-up timescales can be reduced by reducing the range of values of total soil depth, though the relationship between the spin-up time and the maximum available soil moisture (total soil layer depth) is difficult to verify due to a lack of observational data. What is a reasonable value of the total soil layer depth? *Webb et al.* [1993] have compiled a standardized global data set of soil horizon thickness and textures (particle size distributions). The maximum soil depths range from 0.1 m for Lithosol to 8 m for Distric Nitosol in Africa, generally thickest in the well-developed soils of tropical low latitudes and thinnest in the poorly developed soils of high latitudes. However, if bedrock is present within the maximum soil depth, the bottom boundary is located at the depth of the bedrock [e.g., *Abramopoulos et al.*, 1988]. Furthermore, the relationship between profile thickness and soil type differs among the nine major continental divisions. The data used by *Webb et al.* are from a soil taxonomic classification and are questionable as a basis for estimating soil depth, but no better approach is available. Therefore the spatial distribution of soil profile thickness specified in this data set may be preferable to the arbitrary values of total soil layer depth used in most LSMs. *Webb et al.* [1993] have compared estimates of potential storage of water in the soil profile with potential storage of water in the root zone and potential storage of water derived from soil texture. Their results show that the

Table 6. Daytime Mean Values of Aerodynamic and Stomatal Resistances (m/s) Simulated From BATS at Equilibrium for Four Typical Days: January 15, April 15, July 15, and October 15.

		Tropical Forest					Grassland				
		r_a	r_b	r_d	r_s	r_g	r_a	r_b	r_d	r_s	r_g
N	Jan.	21	4	744	183	935	554	72	6554	45547	59
	April	15	3	573	68	679	96	14	1390	3587	55
	July	19	3	646	255	627	154	8	1533	218	657
	Oct.	23	3	639	74	1116	127	12	1582	1707	129
V1	Jan.	16	3	621	156	*	27	5	469	4708	505
	April	12	3	491	62	*	24	5	419	1533	*
	July	14	2	524	214	*	110	6	1158	173	*
	Oct.	20	3	563	66	*	42	5	647	837	*
HFP	Jan.	12	3	608	247	427	444	67	5814	44862	48
	April	14	3	551	70	595	83	13	1268	2967	51
	July	17	3	600	261	686	151	8	1514	218	645
	Oct.	22	3	628	74	1054	113	12	1506	1726	113
HFS	Jan.	58	5	1306	106	2994	1502	94	11016	46912	158
	April	21	3	660	215	967	743	75	7279	25221	82
	July	77	5	1499	122	2673	267	10	2029	497	1105
	Oct.	30	4	728	342	1510	211	15	2127	3584	190
DBR	Jan.	14	3	643	481	582	556	72	6566	45551	60
	April	15	3	559	147	654	96	14	1390	4649	55
	July	20	3	668	519	631	154	8	1534	436	657
	Oct.	23	3	639	148	1116	127	12	1582	2286	129

Values in meters per second. Variable r_a, aerodynamic resistance above canopy; r_b, canopy boundary layer resistance; r_d, aerodynamic resistance between ground and canopy air space; r_s, canopy stomatal resistance; and r_g, aerodynamic resistance between ground and the lowest model level for the barren portion of the ground. Variables r_a, r_b, r_d, r_s, and r_g have been scaled up to a grid square.

*Not applicable.

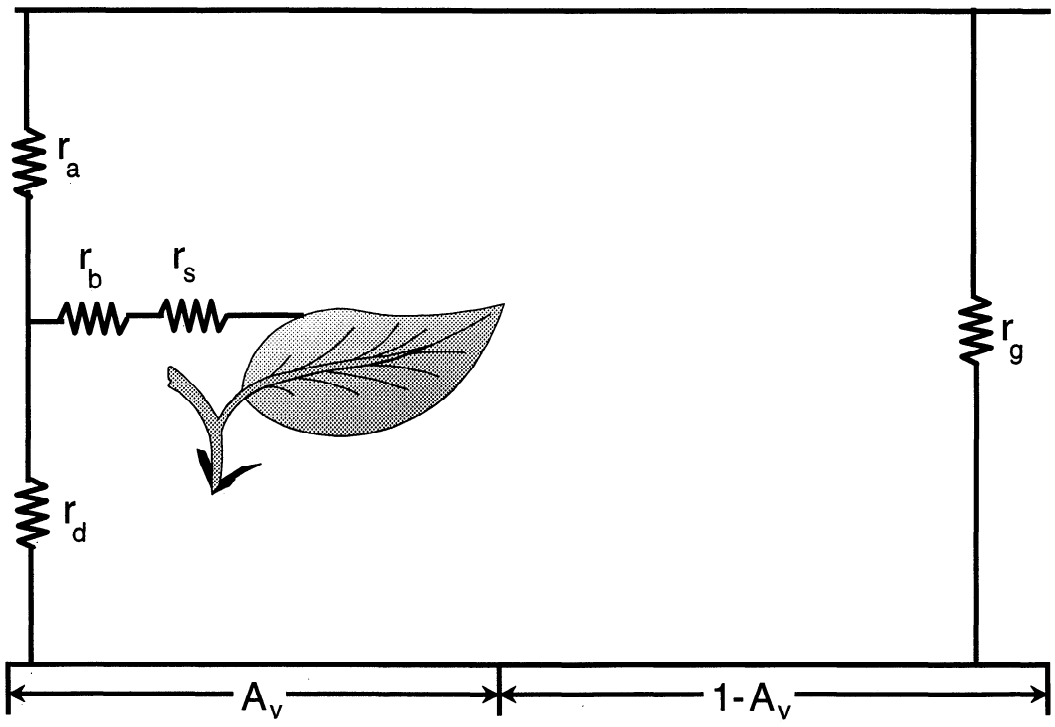

Figure 16. Schematic diagram of the transfer pathways for latent heat flux in BATS. A_v is vegetation cover fraction, r_a is aerodynamic resistance above canopy, r_b is canopy boundary layer resistance, r_d is aerodynamic resistance between ground and canopy air space, r_s is canopy stomatal resistance, and r_g is aerodynamic resistance between ground and the lowest model level for the barren portion of the ground.

zonal mean estimates from the soil profile are the largest of the above three approaches over all the latitudes (see their Figure 3). Using this soil profile in LSMs allows for a more realistic simulation of a change in the hydrological regime needed for global change studies (e.g., climate change induced wetter conditions, more vegetation cover, and deeper roots over current desert areas or climate change induced drier conditions, less vegetation cover and shallower roots over current rainforest areas).

8. Concluding Remarks

This study concentrated on spin-up processes by comparing results from the participating 22 LSMs deduced from the PILPS Phase 1(a) experiments. There is a wide range of spin-up timescales for different models. This study shows that the spin-up time varies linearly with the maximum available soil moisture content in the total soil layer for CTRL and WET, except in those models with a saturated bottom layer, a conclusion that agrees with results from simple bucket models [*Delworth and Manabe*, 1988; *Milly and Dunne*, 1994]. Since most of the 22 schemes are more complex both physically and/or hydrologically, the similarity of the conclusions indicates that even the simple bucket models capture some fundamental spin-up timescales of continental hydrology and that the temporal variability of soil moisture in all these schemes is likely to be governed by a red noise process.

However, the spin-up time increases rapidly as D_w becomes large and this rapidness is greater for NOP than for DRY, a conclusion that can be obtained only through the nonbucket-type models. The nonlinear relationship for the DRY and NOP cases as given in (19) suggests that the nonbucket-type models may cover a much wider spectrum of temporal variability than do the bucket-type models. Therefore the linear relationship between the spin-up time and the maximum available soil moisture established for the bucket models is just a special case for the nonbucket-type models.

In the range of depths considered, there is little apparent linkage between the thickness of the model soil layer below the root zone and total evapotranspiration on timescales up to an annual cycle suggesting that this thickness can be chosen to suit practical situations. In numerical weather prediction models or in four-dimensional data assimilation systems, the effects of soil moisture in any very deep layers may be regarded as negligible, so soil layer below the root zone can be set as desired to a small or even zero thickness to ensure a short spin-up time and efficient computer simulation. However, this layer could become important in long-range climate projections such as interannual variability of climate and climate scenarios due to doubling of CO_2. A more realistic specification of the total soil depth should be based on the global data of vegetation and soil [e.g., *Webb et al.*, 1993]. It may be necessary, but probably not always possible, to differentiate between "weather" and "climate" integrations.

Sensitivity studies using BATS confirmed that precipitation intensity and solar radiation forcing significantly affect the length of the spin-up, while the vegetation cover and stomatal resistance have relatively little effect. However, these latter factors play an important role in modifying the surface water and energy balances.

For most of the models, the initial positive (negative) soil moisture anomalies are associated with positive (negative) changes of latent heat fluxes. Again, this confirms the conclusions obtained from previous work using a very simple land surface model [*Mintz*, 1984; *Yeh et al.*, 1984].

Appendix: Evapotranspiration Components and Resistance Terms

This section, based on that detailed by *Dickinson et al.* [1993], serves to describe the terminologies used in section 6 for BATS. E consists of E_C, evapotranspiration from the vegetated portion of a grid square and E_B, evaporation from the barren portion.

$$E = E_C + E_B . \tag{A1}$$

E_C consists of E_{TR}, transpiration, E_{DEW}, evaporation from intercepted water on canopy surface or interception loss, and E_{UA}, evaporation from ground under canopy.

$$E_C = E_{TR} + E_{DEW} + E_{UA} , \tag{A2}$$

where

$$E_C = \rho_m (q_a - q_m)/r_a , \tag{A3}$$

$$E_{TR} = \rho_m (1 - f_{cw})(LAI/LSAI) (q_c^* - q_a)/(r_b + r_s) , \tag{A4}$$

$$E_{DEW} = \rho_m f_{cw} (q_c^* - q_a)/r_b , \tag{A5}$$

$$E_{UA} = \rho_m \beta_u (q_u^* - q_a)/r_d , \tag{A6}$$

$$E_B = \rho_m \beta_u (q_u^* - q_m)/r_g , \tag{A7}$$

where ρ_m is air density, q_a is the specific humidity of air within canopy air space, q_c^* is the saturated specific humidity of the canopy, and q_u^* is the saturated specific humidity of the ground beneath the canopy. Variables f_{cw} and β_u are wetness factors for canopy surface and soil surface, respectively. Variable r_a is aerodynamic resistance between canopy air space and the lowest model level, r_d is aerodynamic resistance between ground and canopy air space, r_b is aerodynamic resistance between canopy surface and canopy air space, r_g is aerodynamic resistance between ground and the lowest model level, and r_s is canopy stomatal resistance. These resistance terms, as illustrated in Figure 16, are defined as follows

$$r_s = (A_v LAI)^{-1} r_{sl} , \tag{A8}$$

$$r_a = (A_v C_{dh} U_m)^{-1} , \tag{A9}$$

$$r_b = (A_v\, LSAI)^{-1} r_{al}, \quad \text{(A10)}$$

$$r_d = (A_v\, C_d\, U_c)^{-1}, \quad \text{(A11)}$$

$$r_g = [(1 - A_v)\, U_b\, C_{dh}]^{-1}, \quad \text{(A12)}$$

where

$$U_b = (1 - A_v)\, U_m + A_v \{\min(z_{0c}, 1)\, U_c + [1 - \min(z_{0c}, 1)]\, U_m\}, \quad \text{(A13)}$$

$$C_d = 0.004. \quad \text{(A14)}$$

In (A9)-(A13), U_c and U_m are wind speed within canopy and at lowest model level, respectively; C_{dh} is a drag coefficient for land surface; z_{0c} is canopy roughness length; r_{sl} and r_{al} are stomatal and aerodynamic resistance for a leaf, respectively; A_v is the (snow-free) vegetation cover fraction; LAI is leaf area index; $LSAI$ is leaf and stem area index.

Acknowledgments. A large number of people have contributed to this study by providing the results of their model runs for PILPS. They are F. Abramopoulos, R. Avissar, G. Bonan, A. Boone, M. Ek, D. Entekhabi, J. Famiglietti, M. Frech, J. R. Garratt, A. Hahmann, R. Koster, E. Kowalczyk, K. Laval, J. Lean, T. J. Lee, D. Lettenmaier, X. Liang, J.-F. Mahfouf, L. Mahrt, P. C. D. Milly, K. Mitchell, N. de Noblet, J. Noilhan, H.-L. Pan, R. Pielke, A. Robock, C. Rosenzweig, C. A. Schlosser, R. Scott, M. Suarez, S. Thompson, D. Verseghy, P. Wetzel, E. Wood, and Y. Xue. Comments from Adam Schlosser, Parviz Irannejad, Lu Zhang, and especially Chris Milly and an anonymous reviewer were appreciated. Cas Sprout, Brian Auvine, and Margaret Sanderson Rae are thanked for their excellent editorial assistance. This work was completed at the University of Arizona during tenure of a postdoctoral fellowship funded by NOAA project NA16RC0119-01. This is Climatic Impacts Centre publication number 95/16.

References

Abramopoulos, F., C. Rosenzweig, and B. Choudhury, Improved ground hydrology calculations for global climate models (GCMs): Soil water movement and evapotranspiration, *J. Clim., 1,* 921–941, 1988.

Alley, W. M., The Palmer Drought Severity Index: Limitations and assumptions, *J. Clim. Appl. Meteorol., 23,* 1100–1109, 1984.

Chahine, M. T., GEWEX: The global energy and water cycle experiment, *Eos Trans. AGU, 73,* 9,13–14, 1992.

Clapp, R. B., and G. M. Hornberger, Empirical equations for some soil hydraulic properties, *Water Resour. Res., 14,* 601–604, 1978.

Delworth, T. L., and S. Manabe, The influence of potential evaporation on the variabilities of simulated soil wetness and climate, *J. Clim., 1,* 523–547, 1988.

Dickinson, R. E., A. Henderson-Sellers, and P. J. Kennedy, Biosphere atmosphere transfer scheme (BATS) version 1e as coupled to the NCAR community climate model, *NCAR Tech. Note NCAR/TN-387+STR,* 72 pp., Natl. Cent. for Atmos. Res., Boulder, Colo., 1993.

Ducoudre, N. I., K. Laval, and A. Perrier, SECHIBA, a new set of parameterizations of the hydrologic exchanges at the land-atmosphere interface within the LMD atmospheric general circulation model, *J. Clim., 6,* 248–273, 1993.

Entekhabi, D., and P. S. Eagleson, Land surface hydrology parameterization for atmospheric general circulation models including subgrid scale spatial variability, *J. Clim. 2,* 816–831, 1989.

Gates, W. L., AMIP: The atmospheric model intercomparison project, *Bull. Am. Meteorol. Soc., 73,* 1962–1970, 1992.

Henderson-Sellers, A., and R. E. Dickinson, Intercomparison of land surface parameterizations launched, *Eos, Trans. AGU, 73,* 195–196, 1992.

Henderson-Sellers, A., Z.-L. Yang, and R. E. Dickinson, The Project for Intercomparison of Land-surface Parameterization Schemes, *Bull. Am. Meteorol. Soc., 74,* 1335–1349, 1993.

Henderson-Sellers, A., A. J. Pitman, P. K. Love, P. Irannejad, and T. H. Chen, The Project for Intercomparison of Land Surface Parameterization Schemes (PILPS): Phases 2 and 3, *Bull. Am. Meteorol. Soc., 76,* 489–503, 1995.

Huang, J.-Y., and H. Li, *Spectral Analysis in Meteorology* (in Chinese), 318 pp., Meteorological Press, Beijing, 1984.

Hunt, B. G., A model study of some aspects of soil hydrology relevant to climatic modeling, *Q. J. R. Meteorol. Soc., 111,* 1071–1085, 1985.

Idso, S. B., and B. A. Kimball, Tree growth in carbon dioxide enriched air and its implications for global carbon cycling and maximum levels of atmospheric CO_2, *Global Biogeochem. Cycles, 7,* 537–555, 1993.

Koster, R. D., and M. J. Suarez, A comparative analysis of two land surface heterogeneity representations, *J. Clim., 5,* 1379–1390, 1992.

Kowalczyk, E. A., J. R. Garratt, and P. B. Krummel, A soil-canopy scheme for use in a numerical model of the atmosphere – 1D stand-alone model, *CSIRO Tech. Pap. 23,* 56 pp., Commonwealth Sci. and Ind. Res. Org. Div. of Atmos. Res., Melbourne, Victoria, 1991.

Leese, J. A., Implementation plan for the GEWEX Continental-Scale International Project (GCIP), data collection and operational model upgrade, *IGPO Publ. Ser.*, vol. 6, 1993.

Manabe, S., Climate and the ocean circulation, I, The atmospheric circulation and the hydrology of the Earth's surface, *Mon. Weather Rev., 97,* 739–774, 1969.

Milly, P. C. D., and K. A. Dunne, Sensitivity of the global water cycle to the water-holding capacity of land, *J. Clim., 7,* 506–526, 1994.

Mintz, Y., The sensitivity of numerically simulated climate to land-surface boundary conditions, in *The Global Climate,* edited by J. T. Houghton, pp. 79–105, Cambridge Univ. Press, New York, 1984.

Mintz, Y., and G. K. Walker, Global fields of soil moisture and land surface evapotranspiration derived from observed precipitation and surface air temperature, *J. Appl. Meteorol., 32,* 1305–1334, 1993.

Namias, J., Persistence of mid-tropospheric circulations between adjacent months and seasons, in *Rossby Memorial Volume,* pp. 240–248, Rockefeller Institute Press and Oxford Univ. Press, New York, 1958.

Namias, J., Surface-atmosphere interactions as fundamental causes of droughts and other climatic fluctuations, in *Arid Zone Research,* vol. 20, *Changes of Climate Proceedings of Rome Symposium,* pp. 345–359, UNESCO, Paris, 1963.

Noilhan, J., and S. Planton, A simple parameteriztion of land surface processes for meteorological models, *Mon. Weather Rev., 117,* 536–549, 1989.

Palmer, W. C., Meteorological drought, *USWB Res. Pap. 45,* U. S. Weather Bur., Washington, D. C., 1965.

Penman, H. L., Natural evaporation from open water, bare soil and grass, *Proc. R. Soc. London, A, 193,* 120–145, 1948.

Pitman, A. J., Z.-L. Yang, J. G. Cogley, and A. Henderson-Sellers, Description of bare essentials of surface transfer for the Bureau of Meteorology Research Centre AGCM, *BMRC Res. Rep. 32,* 127 pp., Bur. of Meteorol. Res. Cent., Melbourne, Victoria, May 1991.

Pitman, A. J., et al., Project for Intercomparisons of Land Surface Parameterization Schemes (PILPS): Results from off-line control simulations (Phase 1a), *IGPO Publ. Ser.*, vol. 7, 47 pp., December 1993.

Priestley, C. H. B., and R. J. Taylor, On the assessment of surface heat flux and evaporation using large scale parameters, *Mon. Weather Rev., 100,* 81–92, 1972.

Rind, D., R. Goldberg, J. Hansen, C. Rosenzweig, and R. Ruedy, Potential evapotranspiration and the likelihood of future drought, *J. Geophys. Res., 95,* 9983–10,004, 1990.

Robock, A., K. Y. Vinnikov, C. A. Schlosser, N. A. Speranskaya, and Y. Xue, Use of midlatitude soil moisture and meteorological observations to validate soil moisture simulations with biosphere and bucket models, *J. Clim., 8,* 15–35, 1995.

Simmonds, I., and A. H. Lynch, The influence of pre-existing soil moisture content on Australian winter climate, *Int. J. Climatol., 12,* 33–54, 1992.

Trenberth, K. E. (Ed.), *Climate System Modeling,* 788 pp., Cambridge Univ. Press, New York, 1992.

Verseghy, D. L., CLASS – A Canadian Land Surface Scheme for GCMs, I, Soil model, *Int. J. Climatol., 11,* 111–133, 1991.

Webb, R. S., C. E. Rosenzweig, and E. R. Levine, Specifying land surface characteristics in general circulation models: Soil profile data set and derived water-holding capacities, *Global Biogeochem. Cycles, 7,* 97–108, 1993.

Xue, Y., P. J. Sellers, J. L. Kinter, and J. Shukla, A simplified biosphere model for global climate studies, *J. Clim., 4,* 345–364, 1991.

Yeh, T.-C., R. T. Wetherald, and S. Manabe, The effects of soil moisture on the short-term climate and hydrology change – A numerical experiment, *Mon. Weather Rev., 112,* 474–490, 1984.

R. E. Dickinson and Z.-L. Yang, Institute of Atmospheric Physics, PAS Building # 81, University of Arizona, Tucson, AZ 85721. (e-mail: robted@air.atmo.arizona.edu; zly@frost.atmo.arizona.edu)

A. Henderson-Sellers and A. J. Pitman, Climatic Impacts Centre, Macquarie University, North Ryde, New South Wales, 2109, Australia.

(Received July 20, 1994; revised March 15, 1995; accepted March 15, 1995.)